Estimating local outbreak risks and the effects of non-pharmaceutical interventions in age-structured populations: SARS-CoV-2 as a case study

Authors

Francesca A. Lovell-Read[1*], Silvia Shen[1,2], Robin N. Thompson[3,4]

Affiliations

[1]Mathematical Institute, University of Oxford, Oxford, UK

[2]Pembroke College, University of Oxford, Oxford, UK

[3]Mathematics Institute, University of Warwick, Coventry, UK

[4]The Zeeman Institute for Systems Biology and Infectious Disease Epidemiology Research, University of Warwick, Coventry, UK

*** Corresponding author**

Address: Merton College, Merton Street, Oxford, OX1 4JD

E-mail: francesca.lovell-read@merton.ox.ac.uk. Tel: +44 (0)1865 273525.

Abstract

During the COVID-19 pandemic, non-pharmaceutical interventions (NPIs) including school closures, workplace closures and social distancing policies have been employed worldwide to reduce transmission and prevent local outbreaks. However, transmission and the effectiveness of

NPIs depend strongly on age-related factors including heterogeneities in contact patterns and pathophysiology. Here, using SARS-CoV-2 as a case study, we develop a branching process model for assessing the risk that an infectious case arriving in a new location will initiate a local outbreak, accounting for the age-stratification of the host population. We show that the risk of a local outbreak depends on the age of the index case, and we explore the effects of NPIs targeting individuals of different ages. Social distancing policies that reduce contacts outside of schools and workplaces and target individuals of all ages are predicted to reduce local outbreak risks substantially, whereas school closures have a more limited impact. When different NPIs are used in combination, the risk of local outbreaks can be eliminated. We also show that heightened surveillance of infectious individuals reduces the level of NPIs required to prevent local outbreaks, particularly if enhanced surveillance of symptomatic cases is combined with efforts to find and isolate nonsymptomatic infected individuals. Our results reflect real-world experience of the COVID-19 pandemic, during which combinations of intense NPIs have reduced transmission and the risk of local outbreaks. The general modelling framework that we present can be used to estimate local outbreak risks during future epidemics of a range of pathogens, accounting fully for age-related factors.

Keywords

mathematical modelling; infectious disease epidemiology; outbreak probability; SARS-CoV-2; COVID-19; age-structured models; non-pharmaceutical interventions.

1. Introduction

Throughout the COVID-19 pandemic, policy makers worldwide have relied on non-pharmaceutical interventions (NPIs) to limit the spread of SARS-CoV-2. Commonly introduced NPIs have included school closures, workplace closures and population-wide social distancing policies, all of which aim to reduce the numbers of contacts between individuals and disrupt potential chains of transmission [1-4]. Similar measures have previously been adopted for countering other infectious diseases such as Ebola and pandemic influenza [5-7], and are likely to remain a key line of defence against a range of emerging pathogens that are directly transmitted between hosts. NPIs are particularly important when no effective treatment or vaccine is available, and they are also beneficial when vaccination programmes are being rolled out [8-10]. However, the negative economic, social and non-disease health consequences of these interventions have been widely discussed, with the impact of school closures on the academic progress and wellbeing of school-aged individuals a particular concern [7, 11-15]. Therefore, assessing the effectiveness of different NPIs at reducing transmission is critical for determining whether or not they should be used.

Since NPIs such as school and workplace closures affect distinct age groups within the population, when evaluating their effectiveness it is important to account for age-dependent factors that influence transmission. Multiple studies have documented marked heterogeneities in the patterns of contacts between individuals in different age groups, with school-aged individuals tending to have more contacts each day than older individuals [16-22]. Since close contact between individuals is a key driver of transmission for respiratory pathogens such as influenza viruses and SARS-CoV-2, these contact patterns influence transmission dynamics and

67 consequently the effects of interventions that target different age groups [17, 18, 23-26].
68 Additionally, many diseases are characterized by significant age-related variations in
69 pathophysiology. For example, for SARS-CoV-2, children are less susceptible to infection than
70 adults [26-30], and more likely to experience asymptomatic or subclinical courses of infection
71 [27, 30-35]. Since the secondary attack rate (the proportion of close contacts that lead to new
72 infections) from asymptomatic or subclinical hosts is lower than from hosts with clinical
73 symptoms [36-41], children are likely to be less infectious on average than older individuals who
74 are at increased risk of developing symptoms [42-44].
75
76 Previous studies have used age-stratified deterministic transmission models to investigate the
77 effects of NPIs on COVID-19 epidemic peak incidence and timing. Prem *et al.* [45] projected the
78 outbreak in Wuhan, China, over a one year period under different control scenarios, and
79 demonstrated that a period of intense control measures including school closures, a 90%
80 reduction in the workforce and a significant reduction in other social mixing could delay the
81 epidemic peak by several months. Zhang *et al.* [26] predicted that eliminating all school contacts
82 during the outbreak period would lead to a noticeable decrease in the peak incidence and a later
83 peak; however, they did not take differences between symptomatic and asymptomatic cases into
84 account explicitly. In contrast, Davies *et al.* [30] used estimates of age-dependent susceptibility
85 and clinical fraction fitted to the observed age distribution of cases in six countries to
86 demonstrate that school closures alone were unlikely to reduce SARS-CoV-2 transmission
87 substantially. Davies *et al.* [46] subsequently concluded that a combination of several strongly
88 enforced NPIs would be necessary to avoid COVID-19 cases exceeding available healthcare
89 capacity in the UK.

90

91 Rather than considering the entire epidemic curve, here we focus on estimating the probability
92 that cases introduced to a new location trigger a local outbreak as opposed to fading out with few
93 cases. Localised clusters of transmission have been a feature of the COVID-19 pandemic [47-
94 49], and assessing the risk that such local outbreaks occur requires a stochastic model in which
95 the pathogen can either invade or fade out. Stochastic branching process models have been
96 applied previously to assess outbreak risks for different pathogens in age-homogeneous
97 populations [50-54] and populations in which adults and children are considered as two distinct
98 groups [55]. However, the significant heterogeneities in contacts patterns and pathophysiology
99 between individuals across the full range of ages have never previously been considered in
100 estimates of local outbreak risks. Here, we develop an age-structured branching process model
101 that can be used to estimate the probability of a local outbreak occurring for index cases of
102 different ages, and demonstrate how the age-dependent risk profile changes when susceptibility
103 to infection and clinical fraction vary with age.
104

105 We use the model to investigate the effects on the local outbreak probability of NPIs that aim to
106 reduce the numbers of contacts between individuals. Specifically, we use location-specific
107 contact data detailing the average numbers of daily contacts occurring in school, in the
108 workplace and elsewhere [16] to model the impacts of school closures, workplace closures and
109 broader social distancing policies. We demonstrate that, for SARS-CoV-2, contacts occurring
110 outside schools and the workplace are a key driver of sustained transmission. Thus, population-
111 wide social distancing policies that affect individuals of all ages lead to a substantial reduction in
112 the risk of local outbreaks. In contrast, since school-aged individuals only make up around one

quarter of the UK population and tend to have large numbers of contacts outside school, school closures are predicted to have only a limited effect when applied as the sole NPI.

We then go on to consider the impacts of mixed strategies made up of multiple NPIs, as well as additional NPIs that do not simply reduce numbers of contacts. Specifically, we show that rigorous surveillance and effective isolation of infected hosts can reduce the level of contact-reducing NPIs required to achieve substantial reductions in the risk of local outbreaks. Although we use SARS-CoV-2 as a case study, our approach can be applied more generally to explore the effects of NPIs on the risk of outbreaks of any pathogen for which age-related heterogeneities play a significant role in transmission dynamics.

2. Methods

2.1 Model

We considered a branching process model in which the population was divided into 16 age groups, denoted $G_1, G_2, \ldots, G_{16}$. The first 15 groups represent individuals aged 0-74, divided into five-year intervals (0-4, 5-9, 10-14 etc.). The final group represents individuals aged 75 and over. The total number of individuals in age group G_k is denoted N_k. Infected individuals in each age group G_k are classified into compartments representing asymptomatic (A_k), presymptomatic (P_k) or symptomatic (S_k) hosts, where an individual in the A_k compartment does not develop symptoms at any time during their course of infection.

An infected individual of any type in group G_k may generate new infections in any age group. In our model, the rate at which a single infected symptomatic individual in group G_k generates infections in group G_j is given by

$$\beta_{kj} = B\tau_k\omega_j C_{kj}.$$

Here, τ_k represents the infectivity of individuals in group G_k, ω_j represents the susceptibility to infection of individuals in group G_j, C_{kj} represents the daily number of unique contacts a single individual in group G_k has with individuals in group G_j, and B is a scaling factor that can be used to set the reproduction number of the pathogen being considered (see Section 2.2). Since the initial phase of potential local outbreaks are the focus of this study, we did not account for depletion of susceptible hosts explicitly. The relative transmission rates from presymptomatic and asymptomatic individuals compared to symptomatic individuals are given by the scaled quantities $\eta\beta_{kj}$ and $\theta\beta_{kj}$, respectively, where η and θ were chosen so that the proportions of transmissions generated by presymptomatic and asymptomatic hosts were in line with literature estimates [56]. The parameter ξ_k represents the proportion of asymptomatic infections in group G_k, so that a new infection in group G_k either increases A_k by one (with probability ξ_k) or increases P_k by one (with probability $1 - \xi_k$).

A presymptomatic individual in group G_k may go on to develop symptoms (transition from P_k to S_k) or be detected and isolated (so that P_k decreases by one). A symptomatic individual in group G_k may be detected and isolated as a result of successful surveillance, or may be removed due to self-isolation, recovery or death (so that S_k decreases by one in either case). Similarly, an asymptomatic individual in group G_k may be detected and isolated or recover (so that A_k decreases by one). A schematic of the different possible events in the model is shown in Fig 1.

The parameter λ represents the rate at which presymptomatic individuals develop symptoms, so that the expected duration of the presymptomatic infectious period is $1/\lambda$ days in the absence of surveillance of nonsymptomatic infected individuals. Similarly, the expected duration of the asymptomatic infectious period in the absence of surveillance is $1/\nu$ days. The parameter μ represents the rate at which symptomatic individuals are removed as a result of self-isolation, recovery or death, so that the duration of time for which they are able to infect others is $1/\mu$ days.

For each group G_k, the rate at which symptomatic individuals are detected and isolated as a result of enhanced surveillance is determined by the parameter ρ_k. Analogously, the parameter σ_k governs the rate at which presymptomatic and asymptomatic individuals in G_k are detected and isolated. We assumed that surveillance measures targeted towards nonsymptomatic hosts are equally effective for those who are presymptomatic and those who are asymptomatic, and therefore used the same rate of isolation due to surveillance for both of these groups.

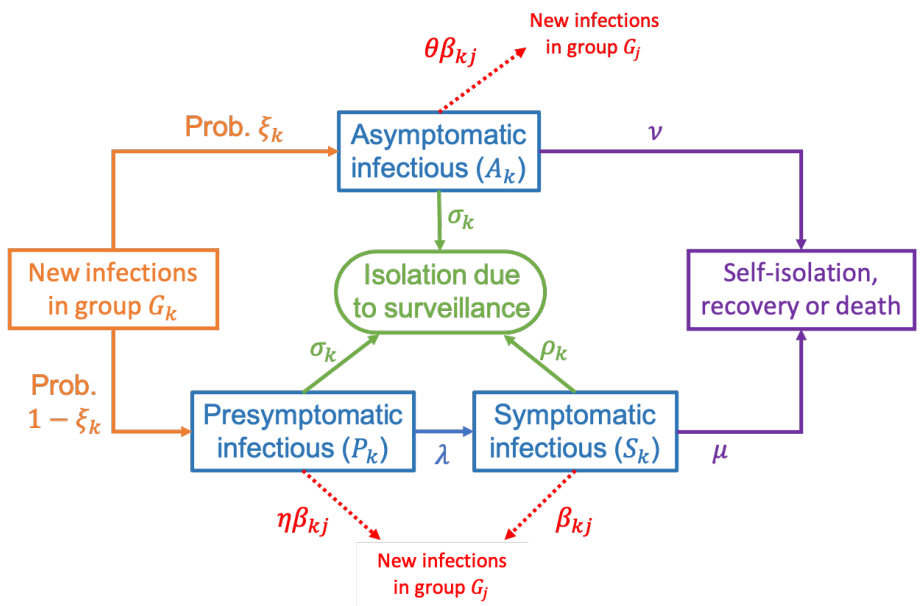

Fig 1. The branching process model used in our analyses. Schematic showing the different possible events in the branching process model and the rates at which they occur. The parameters of the model are described in the text and in Tables 1, 2 and 3.

2.2 Reproduction number

The effective reproduction number, R, represents the expected number of secondary infections generated by a single infected individual during their entire course of infection, accounting for interventions that are in place:

$$R = \sum_{k=1}^{16} \frac{N_k}{N} \sum_{l=1}^{16} \left[\frac{\xi_k \theta \beta_{kl}}{\nu + \sigma_k} + (1-\xi_k)\left(\frac{\eta \beta_{kl}}{\lambda + \sigma_k} + \frac{\lambda}{\lambda + \sigma_k} \frac{\beta_{kl}}{\mu + \rho_k} \right) \right], \quad (1)$$

where $N = N_1 + \cdots + N_{16}$ is the total population size. This expression is an average of the expected number of secondary infections generated by individuals in each age group, weighted by the proportions of the population belonging to each age group. This corresponds to the assumption that the initial infected host is more likely to belong to an age group containing more individuals than an age group with fewer individuals. For an individual in age group G_k, the

expected number of secondary infections is the sum of the expected number of transmissions from a host who begins in the asymptomatic class and a host who begins in the presymptomatic class, respectively weighted by the probabilities ξ_k and $1 - \xi_k$ that an infected host experiences an asymptomatic or a symptomatic course of infection. Transmissions arising from a host who begins in the presymptomatic class comprise those which occur during the presymptomatic period and those which occur during the symptomatic period, accounting for the possibility that the individual is isolated before developing symptoms. In the absence of interventions, i.e. when $\sigma_k = \rho_k = 0$ (representing no enhanced isolation as a result of surveillance) and β_{kl} is calculated using contact patterns that are characteristic of normal behaviour, the effective reproduction number, R, is equal to the basic reproduction number, R_0.

2.3 Model parameterisation

The numbers of individuals in each age group (values of N_k) were chosen according to age demographic data from the United Nations 2020 global population forecasts for the UK [57] (Fig 2A). The daily numbers of contacts between individuals in each age group (values of C_{kj}) were set according to the 16x16 'contact matrix' for the UK, in which the (k, j)th entry represents the expected daily number of unique contacts an individual in age group G_k has with individuals in age group G_j [16]. In addition to matrices representing 'all' contacts (Figure 2B), we also considered matrices detailing a breakdown into 'school', 'work', 'home' and 'other' contacts (Figures 2C-F), allowing us to investigate the effects of control interventions that reduce contacts in each of these settings.

Since we considered SARS-CoV-2 as a case study, we used studies conducted during the COVID-19 pandemic to inform the epidemiological parameters of our model. Despite previous research assessing the relationships between age and factors such as susceptibility to SARS-CoV-2 infection or the propensity to develop symptoms, there is some variation in estimated parameters between different studies. To test the robustness of our results to this uncertainty, we conducted our analyses under three different scenarios (A, B and C). In scenario A, we assumed that susceptibility to infection (values of ω_k) and the proportion of hosts who experience a fully asymptomatic course of infection (values of ξ_k) are independent of age. In scenario B, susceptibility was assumed to vary with age but the proportion of asymptomatic infections is independent of age. In scenario C, we allowed both susceptibility and the asymptomatic proportion to vary with age. The values used for the parameters ω_k and ξ_k in each of these three scenarios are shown in Table 1 (see also [30]).

In all scenarios considered, the inherent infectivity was not assumed to be age-dependent (i.e. $\tau_k = 1$ for all values of k). In other words, the expected infectiousness of infected hosts in different age groups was governed solely by the proportion of asymptomatic infections in that age group. We chose the scaling factors η and θ for the relative transmission rates from presymptomatic and asymptomatic individuals compared to symptomatic individuals so that the proportions of infections arising from each of these groups were in line with literature estimates (see Table 3 and [56]).

In the absence of enhanced isolation, we set the expected duration of the presymptomatic infectious period and the time for which symptomatic individuals are able to infect others to be

232 $1/\lambda = 2$ days and $1/\mu = 8$ days, respectively [58-61]. The asymptomatic infectious period was
233 then chosen so that all infected individuals are expected to be infectious for the same period (i.e.
234 $1/\nu = 10$ days). Initially, we set the isolation rates ρ_k and σ_k equal to 0 for all k; later, we
235 considered the effects of increasing these rates.
236
237 Initially, we fixed $R_0 = 3$ [62-65] and used expression (1) to determine the appropriate
238 corresponding value of the scaling factor B. Later, when considering the impact of NPIs on the
239 probability of a local outbreak, we retained this value of B and used expression (1) to determine
240 how the reproduction number changes as a result of the control implemented.
241
242 **Table 1. Baseline values of age-dependent parameters.** Values used for the age-dependent relative
243 susceptibility to infection (ω_k) and the proportion of infections that are asymptomatic (ξ_k) for each of the
244 scenarios A, B and C [30].

Age group (G_k)	Relative susceptibility (ω_k)		Asymptomatic proportion (ξ_k)	
	Scenario A	Scenarios B & C	Scenarios A & B	Scenario C
G_1, G_2 (0-9)	1.0	0.4	0.584 (weighted average of age-dependent values of ξ_k in Scenario C)	0.71
G_3, G_4 (10-19)		0.38		0.79
G_5, G_6 (20-29)		0.79		0.73
G_7, G_8 (30-39)		0.86		0.67
G_9, G_{10} (40-49)		0.8		0.6
G_{11}, G_{12} (50-59)		0.82		0.51
G_{13}, G_{14} (60-69)		0.88		0.37
G_{15}, G_{16} (70+)		0.74		0.31

245
246 **Table 2. Baseline values of scenario-independent parameters.** Values used for the parameters that did not
247 vary between scenarios A, B and C. We also considered strategies involving enhanced surveillance ($\rho_k, \sigma_k >$
248 0) – see Fig 6.

Parameter	Meaning	Baseline value	Justification
R_0	Expected number of secondary infections generated by a single	$R_0 = 3$	Within estimated range for SARS-CoV-2 [62-65]

	infectious host in the absence of interventions		
λ	Rate at which presymptomatic hosts develop symptoms	$\lambda = 1/2 \text{ days}^{-1}$	[58]
μ	Rate at which symptomatic hosts are removed due to self-isolation, recovery or death	$\mu = 1/8 \text{ days}^{-1}$	[59-61]
ν	Rate at which asymptomatic hosts are removed due to recovery or death	$\nu = 1/10 \text{ days}^{-1}$	Chosen so that, in the absence of interventions, the expected duration of infection is identical for all infected hosts $\left(\frac{1}{\nu} = \frac{1}{\lambda} + \frac{1}{\mu}\right)$
τ_k	(Relative) infectivity parameter	$\tau_k = 1$ for $k = 1, \dots, 16$	Assumed
ρ_k	Isolation rate due to surveillance of symptomatic individuals	$\rho_k = 0$ for $k = 1, \dots, 16$	N/A
σ_k	Isolation rate due to surveillance of nonsymptomatic individuals	$\sigma_k = 0$ for $k = 1, \dots, 16$	N/A

Table 3. Baseline values of scenario-dependent scaling parameters. Values used for the scaling parameters B, η and θ for each of the scenarios A, B and C.

Parameter	Meaning	Value			Justification
		Scenario A	Scenario B	Scenario C	
B	Transmission rate scaling factor	0.0386	0.0559	0.0607	Chosen so that $R_0 = 3$ [62-65]
η	Relative transmission rate of presymptomatic hosts compared to symptomatic hosts	4.83	4.83	4.83	Chosen so that the proportion of all infections arising from presymptomatic hosts is 0.489 [56]
θ	Relative transmission rate of asymptomatic hosts compared to symptomatic hosts	0.149	0.149	0.130	Chosen so that the proportion of all infections arising from asymptomatic hosts is 0.106 [56]

2.4 Probability of a local outbreak

The probability that an infected individual in a particular age group initiates a local outbreak when they are introduced into the population was calculated using the branching process model, as follows.

The probability of a local outbreak not occurring (i.e. pathogen fadeout occurs), starting from a single symptomatic (or presymptomatic, asymptomatic respectively) infectious individual in age group G_k was denoted by x_k (y_k, z_k). Beginning with a single symptomatic individual in G_k, the possibilities for the next event are as follows:

1. The infected individual in G_k infects a susceptible individual in G_j, so that either A_j increases by one (with probability ξ_j) or P_j increases by one (with probability $(1-\xi_j)$. This occurs with probability

$$\alpha_{kj} = \frac{\beta_{kj}}{\mu + \rho_k + \sum_{l=1}^{16} \beta_{kl}}.$$

2. The infected individual in G_k recovers, dies or is isolated before infecting anyone else, so that S_k decreases to zero (and there are no infected individuals left in the population). This occurs with probability

$$\gamma_k = \frac{\mu + \rho_k}{\mu + \rho_k + \sum_{l=1}^{16} \beta_{kl}}.$$

If there are no infectious hosts present in the population, then a local outbreak will not occur. Therefore, assuming that chains of transmission arising from infectious individuals are independent, the probability that no local outbreak occurs beginning from a single symptomatic individual in G_k is

$$x_k = x_k \left[\sum_{j=1}^{16} \alpha_{kj} \left(\xi_j z_j + (1-\xi_j) y_j \right) \right] + \gamma_k. \quad (2)$$

Similarly, beginning instead with a single presymptomatic individual in G_k, the possibilities for the next event are:

1. The presymptomatic infected individual in G_k infects a susceptible individual in G_j, so that as before either A_j increases by one (with probability ξ_j) or P_j increases by one (with probability $(1-\xi_j)$. This occurs with probability

$$\tilde{\alpha}_{kj} = \frac{\eta\beta_{kj}}{\lambda + \sigma_k + \eta\sum_{l=1}^{16}\beta_{kl}}.$$

2. The infected individual in G_k develops symptoms (transitions from P_k to S_k). This occurs with probability

$$\delta_k = \frac{\lambda}{\lambda + \sigma_k + \eta\sum_{l=1}^{16}\beta_{kl}}.$$

3. The infected individual in G_k is isolated before infecting anyone else, so that S_k decreases by one. This occurs with probability

$$\phi_k = \frac{\sigma_k}{\lambda + \sigma_k + \eta\sum_{l=1}^{16}\beta_{kl}}.$$

Therefore, the probability that no local outbreak occurs beginning from a single presymptomatic individual in G_k is

$$y_k = y_k\left[\sum_{j=1}^{16}\tilde{\alpha}_{kj}\left(\xi_j z_j + \left(1-\xi_j\right)y_j\right)\right] + \delta_k x_k + \phi_k. \quad (3)$$

Similarly, the probability z_k that a local outbreak does not occur starting from a single asymptomatic individual in G_k satisfies the equation

$$z_k = z_k\left[\sum_{j=1}^{16}\hat{\alpha}_{kj}\left(\xi_j z_j + \left(1-\xi_j\right)y_j\right)\right] + \epsilon_k, \quad (4)$$

where

$$\hat{\alpha}_{kj} = \frac{\theta\beta_{kj}}{\nu + \sigma_k + \theta\sum_{l=1}^{16}\beta_{kl}} \quad \text{and} \quad \epsilon_k = \frac{\nu + \sigma_k}{\nu + \sigma_k + \theta\sum_{l=1}^{16}\beta_{kl}}.$$

The system of simultaneous equations $(2) - (4)$ can be solved numerically to obtain x_k, y_k and z_k (specifically, we take the minimal non-negative solution, as is standard when calculating extinction probabilities using branching process models [54, 66]). Then, for each k, the probability of a local outbreak occurring beginning from a single symptomatic (or presymptomatic, asymptomatic respectively) individual in group G_k is given by $1 - x_k$ $(1 - y_k, 1 - z_k)$.

Throughout, we consider the probability p_k of a local outbreak occurring beginning from a single nonsymptomatic individual in group G_k arriving in the population at the beginning of their infection:

$$p_k = \xi_k(1 - z_k) + (1 - \xi_k)(1 - y_k).$$

The average local outbreak probability, P, which is defined as the probability of a local outbreak when the index case is chosen randomly from the population, is also considered. The value of P is therefore a weighted average of the p_k values, where the weights correspond to the proportion of the population represented by each group:

$$P = \frac{1}{N}\sum_{k=1}^{16} N_k p_k.$$

This reflects an assumption that the index case is more likely to come from an age group with more individuals than an age group with fewer individuals.

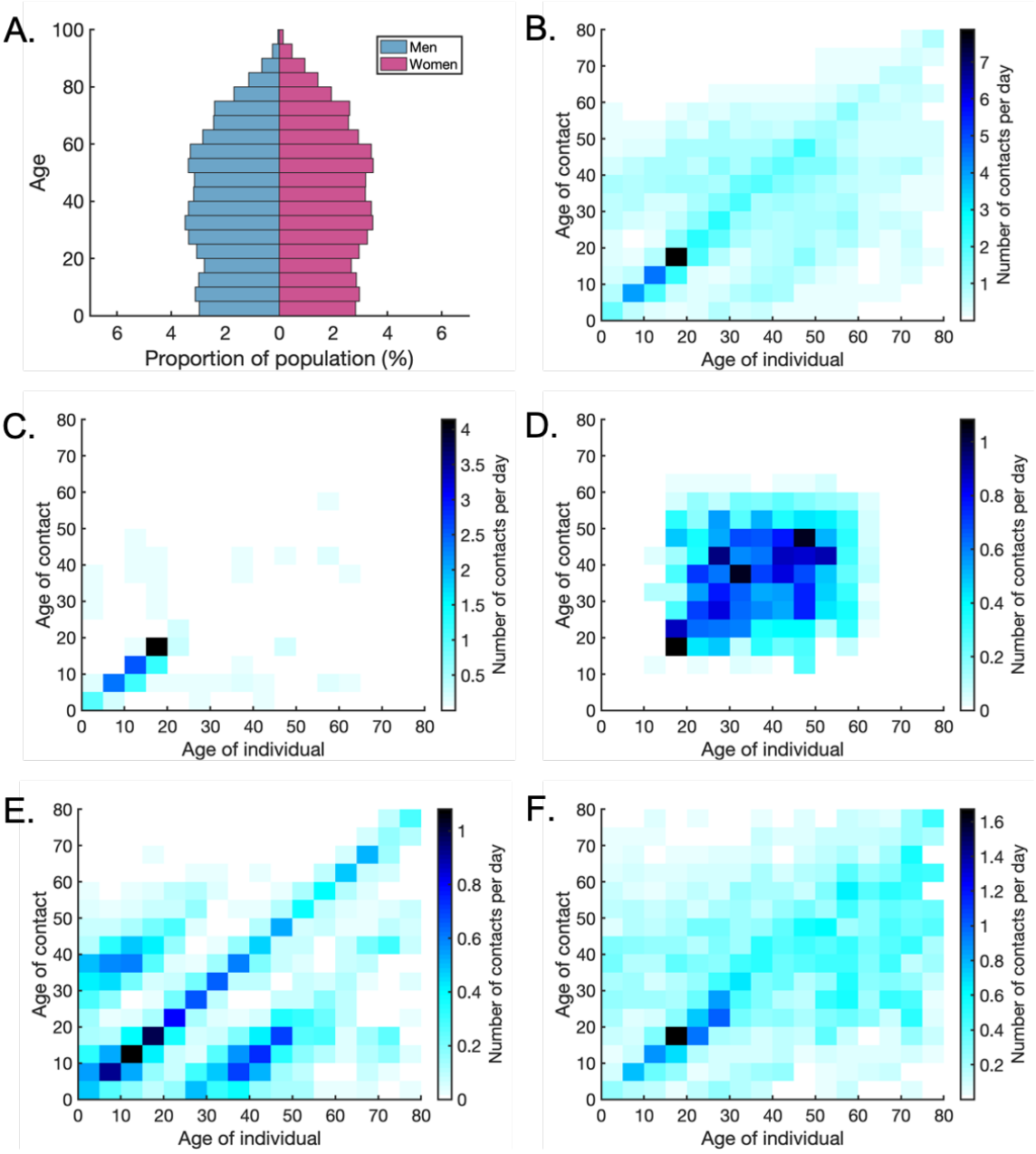

Fig 2. Age demographic and age-structured contact patterns for the United Kingdom. A. United Nations projected UK 2020 population size split into five-year age groups [57]. B. Heat map of UK 'all contacts' matrix, representing the expected daily number of unique contacts that an individual in each age group G_k has with individuals in each other age group G_j [16]. C. The analogous figure to B, but showing only the subset of 'all' contacts that occur in schools ('school' contacts). D. The analogous figure to C, but showing only 'workplace' contacts. E. The analogous

figure to C, but showing only 'home' contacts. F. The analogous figure to C, but showing only 'other' contacts (i.e. all contacts outside schools, workplaces or homes).

3. Results

3.1 Effect of the age of the index case on the risk of a local outbreak

We first considered the probability that a single infected individual in a particular age group G_k initiates a local outbreak when introduced into a new host population. This quantity was calculated for each of the three scenarios A, B and C (Fig 3).

In scenario A, the variation in the outbreak risk for introduced cases of different ages is driven solely by the numbers of contacts between age groups. As a result, due to their higher numbers of daily contacts, school- and working-age individuals are more likely to trigger an outbreak than children under five or adults over 60, with index cases aged 15-19 posing the highest risk (0.596) (Fig 3A). These findings do not change significantly when susceptibility is allowed to vary with age in scenario B (Fig 3B). However, in scenario C, assuming that the clinical fraction also varies between age groups significantly alters the age-dependent risk profile. This is because asymptomatic individuals are assumed to be less infectious than symptomatic individuals, and therefore an index case in an age group with a high proportion of asymptomatic infections is less likely to trigger a local outbreak. In this scenario, index cases aged 40 or over had a disproportionately high probability of generating a local outbreak, with individuals aged 70-74 presenting the highest risk (0.598). These older individuals are more likely to develop symptoms than younger individuals (Table 1), leading to a higher expected infectiousness. In contrast, individuals below the age of 40 had a below average probability of generating a local outbreak, with individuals aged 10-14 presenting the lowest risk (0.284). Noticeably, individuals aged 5-

347 19 presented relatively low risks, despite the high numbers of contacts occurring among these
348 age groups (Fig 2B). In this scenario, the large number of contacts was offset by the fact that
349 individuals in these age groups are more likely to be asymptomatic and consequently less
350 infectious than older individuals (Table 1). Therefore, an index case in one of these age groups is
351 likely to lead to fewer secondary transmissions. Furthermore, the contact patterns between
352 individuals in these age groups are highly assortative with respect to age (Fig 2B). Therefore, in
353 addition to the index case being less infectious, a high proportion of the contacts they make are
354 with individuals who are also likely to be less infectious, as well as being less susceptible to
355 infection in the first place.
356
357 We performed our subsequent analyses for each of the three scenarios A, B and C, with
358 qualitatively similar results. The figures shown in the main text are for scenario C, since we
359 deem this scenario to be the most realistic for SARS-CoV-2 transmission, but the analogous
360 results for scenarios A and B are presented in Supplementary Figs S1-6.
361

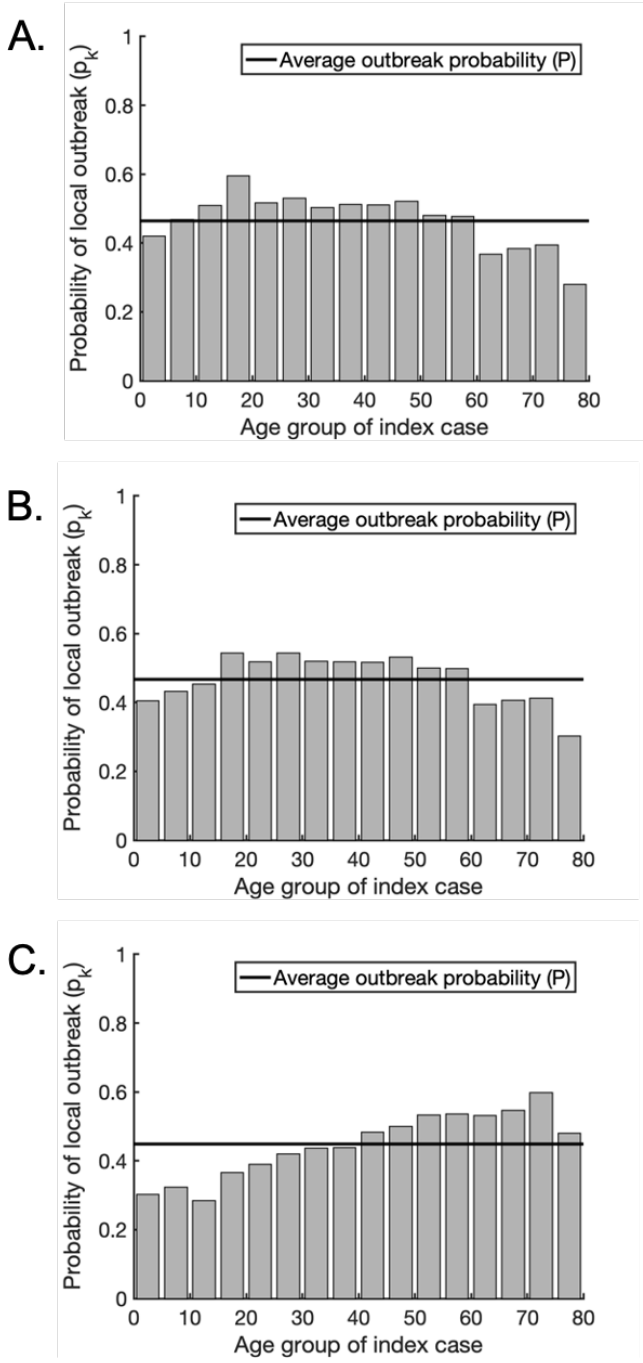

Fig 3. The probability of a local outbreak depends on the age of the index case. A. The probability that a single infected individual in any given age group triggers a local outbreak (grey bars) for scenario A, in which susceptibility and clinical fraction are assumed constant across all age groups. The weighted average local outbreak probability *P* is shown by the black horizontal line. B. The analogous figure to A but for scenario B, in which clinical fraction is assumed constant across

all age groups but susceptibility varies with age (Table 1). C. The analogous figure to A but for scenario C, in which both susceptibility and clinical fraction vary with age (Table 1).

3.2 Effect of the target age group on NPI effectiveness

We next considered the effects of NPIs that reduce the number of contacts between individuals on the probability that an introduced case will lead to a local outbreak. To approximate the relative effects of school closures, workplace closures and population-wide social distancing policies, we calculated the age-dependent risk profiles when each of these types of contact were excluded from the overall contact matrix.

First, we removed all 'school' contacts from the total contact matrix (Fig 4A). For scenario C, removing 'school' contacts led to a 4.2% reduction in the average probability of a local outbreak, from 0.449 to 0.430. This small reduction is unsurprising for scenario C, since in that scenario school-aged infected individuals are assumed more likely to be asymptomatic than other infected individuals, and therefore their expected infectiousness is lower. However, even for scenarios A and B, in which school-aged individuals present the greatest risk of triggering an outbreak, the effectiveness of removing 'school' contacts alone at reducing the local outbreak probability was limited (reductions of 7.2% and 4.75% respectively; see Supplementary Figs S1A, S4A). In each scenario, the reduction in risk was predominantly for school-aged index cases, with the risk from index cases of other ages only slightly reduced. Second, we considered the effects of removing 'work' contacts from the total contact matrix (Fig 4B). This led to a more substantial 25.4% reduction in the average probability of a local outbreak for scenario C (with corresponding reductions of 19.0% and 24.0% for scenarios A and B respectively; see Supplementary Figs S1B, S4B). As well as reducing the risk of an outbreak from an index case of working age, removing

392 ‘work’ contacts also reduced the probability of a local outbreak occurring starting from a school-
393 aged individual. This is because closing workplaces helps to block chains of transmission that
394 begin with an infected child. For example, a transmission chain involving a child transmitting to
395 an adult at home, followed by subsequent spread around the adult’s workplace, will be less likely
396 to occur. Third, we investigated the effect of removing all ‘other’ contacts, reflecting perfect
397 social distancing being observed outside of the home, school or workplace (Fig 4C). This had the
398 most significant effect of the three types of contact-reducing intervention considered, reducing
399 the probability of a local outbreak by 41.7% for scenario C (and 30.7% or 33.2% for scenarios A
400 and B, respectively).
401
402 In the three cases described above, we considered complete reductions in ‘school’, ‘work’ and
403 ‘other’ contacts, respectively. In practice, such complete elimination of contacts is unfeasible.
404 We therefore also considered partial reductions in ‘school’, ‘work’ and ‘other’ contacts, and
405 compared the resulting reductions in the local outbreak probability (Fig 4D). For any given
406 percentage reduction in contacts, reducing ‘other’ contacts always led to the largest reduction in
407 the local outbreak probability (see also Supplementary Figs S1D, S4D). This suggests that
408 reducing social contacts outside schools and workplaces can be an important component of
409 strategies to reduce the risk of local outbreaks of SARS-CoV-2. However, this alone is not
410 enough to eliminate the risk of local outbreaks entirely. For greater risk reductions using contact-
411 reducing NPIs, a mixed approach involving combinations of reductions in ‘school’, ‘workplace’
412 and ‘other’ contacts is needed.
413

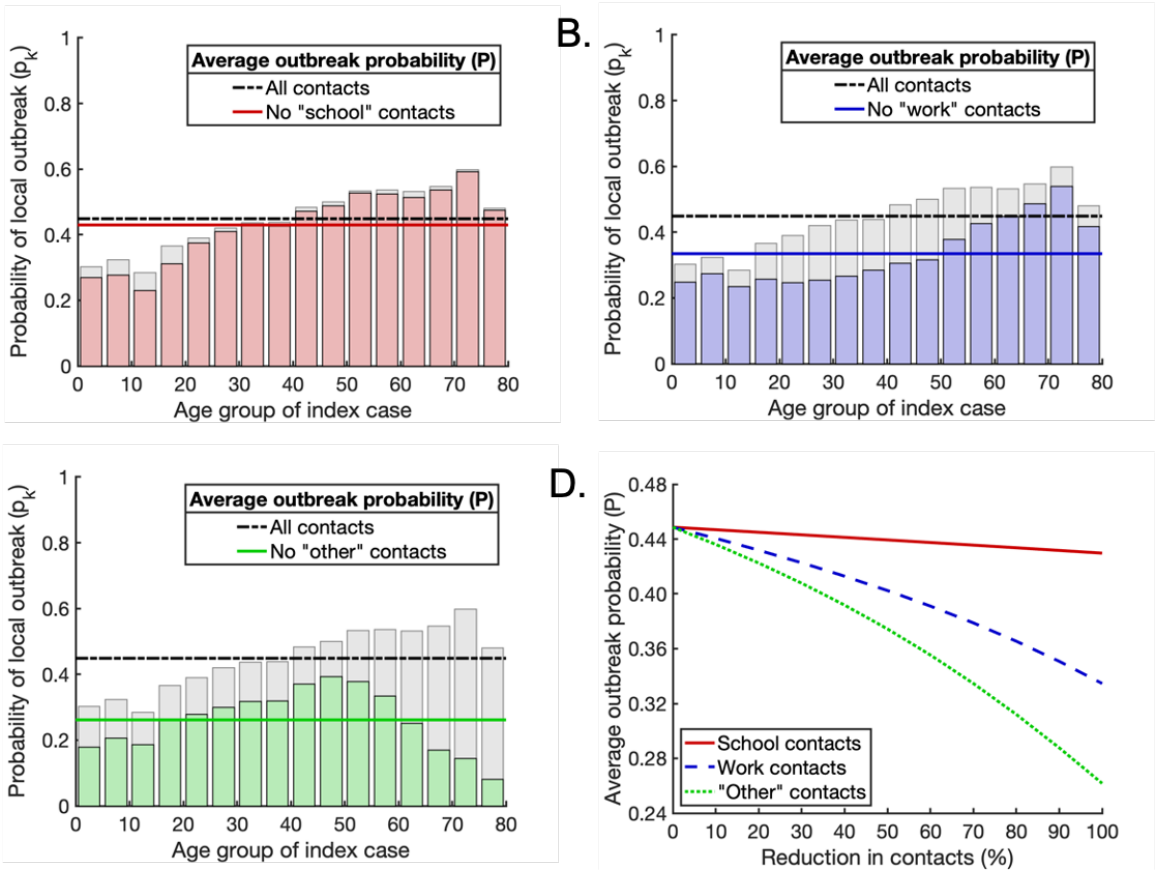

Fig 4. The effects of interventions that reduce contacts between individuals on the probability of a local outbreak. A. The effect of removing all 'school' contacts on the probability of a local outbreak. Pale grey bars and black dash-dotted line represent the local outbreak probabilities without any contacts removed (as in Fig 3C). Red bars and the solid red line represent the local outbreak probabilities and their weighted average when 'school' contacts are removed. B. The analogous figure to A, but with all 'work' contacts removed. C. The analogous figure to A, but with all 'other' contacts removed. D. Partial reductions in 'school', 'work' and 'other' contacts, and the resulting reductions in the average local outbreak probability (solid red, dashed blue and dotted green lines respectively).

3.3 Mixed strategies for reducing the local outbreak risk

Next, we considered the effects of combining reductions in 'school', 'work' and 'other' contacts on the local outbreak probability (Fig 5; analogous results for scenarios A and B are shown in

427 Supplementary Figs S2 and S5). We allowed reductions in ‘school’ and ‘work’ contacts to vary
428 between 0% and 100% whilst ‘other’ contacts were reduced by 25%, 50% or 75% (Fig 5A,B,C,
429 respectively).
430
431 Since NPIs have negative economic, social and non-disease health consequences, policy makers
432 may choose to implement public health measures in which the risk of local outbreaks is not
433 eliminated completely. These results allow mixed strategies to be determined in which the local
434 outbreak probability is reduced to a pre-specified ‘acceptable’ level. For example, to reduce the
435 outbreak probability to 0.25, ‘other’ contacts can be reduced by 25% from the baseline level, and
436 ‘school’ and ‘home’ contacts reduced as indicated by the red dotted contour marked ‘0.25’ in Fig
437 5A. Alternatively, to achieve the same local outbreak risk, ‘other’ contacts can instead be
438 reduced by 50% or by 75% with the degree of ‘school’ and ‘work’ reductions chosen according
439 to the contours marked ‘0.25’ in Figs 5B,C respectively.
440
441 If a policy maker wishes to eliminate the local outbreak risk entirely using contact-reducing
442 NPIs, very significant reductions in multiple types of contacts are needed in combination. For
443 example, even if all ‘school’ and ‘work’ contacts are removed, ‘other’ contacts must be reduced
444 by 66% for the overall average local outbreak probability to fall below 0.01 (Fig 5D). Since such
445 substantial reductions in multiple types of contacts are unlikely to be possible, this suggests that
446 contact-reducing NPIs must be combined with other interventions, such as effective surveillance
447 and isolation strategies, to eliminate local outbreaks.
448

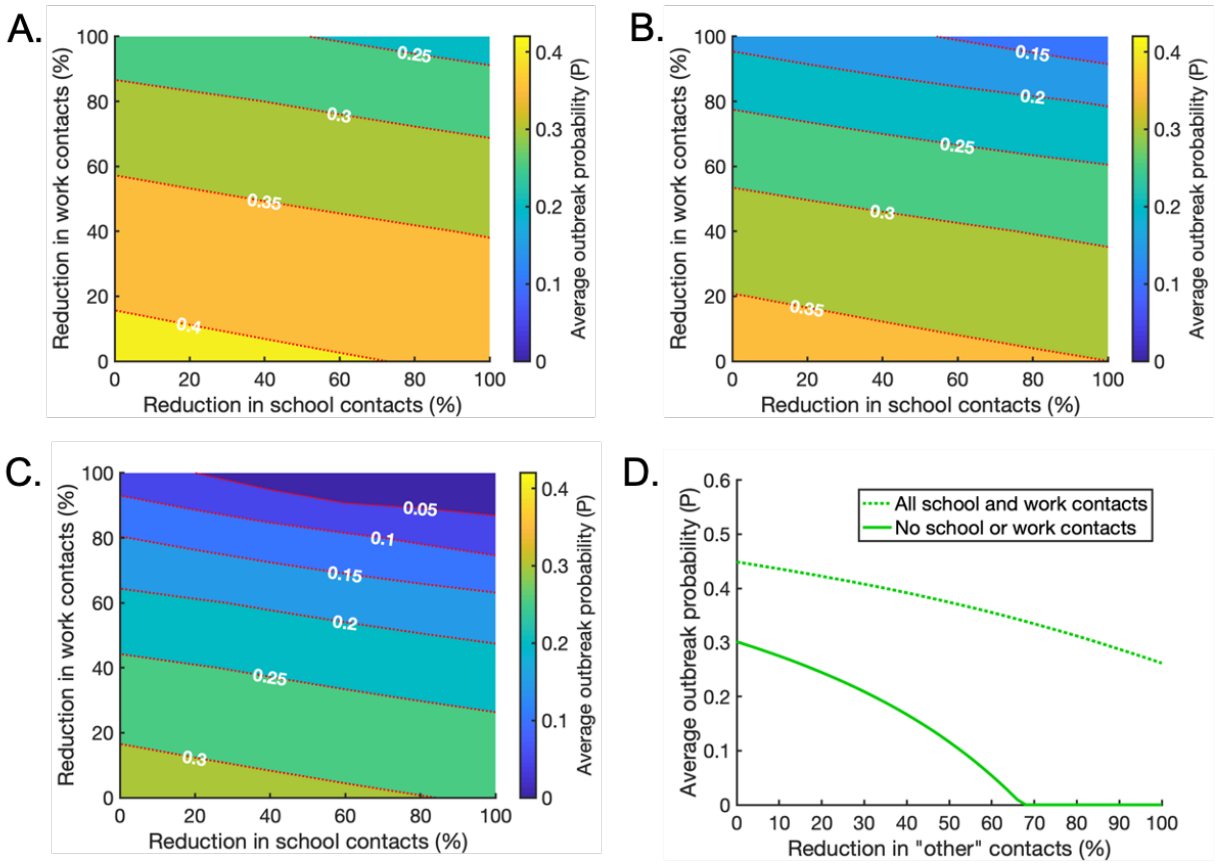

Fig 5. The effects of intervention strategies that combine reductions in 'school', 'work' and 'other' contacts. A. The effect of reducing 'school' and 'work' contacts on the weighted average probability of a local outbreak (*P*), when 'other' contacts are reduced by 25% across all age groups. Red dotted lines indicate contours along which the local outbreak probability is constant. B. The analogous figure to A, but with a 50% reduction in 'other' contacts. C. The analogous figure to A, but with a 75% reduction in 'other' contacts. D. The effect of reducing 'other' contacts on the average local outbreak probability when 'school' and 'work' contacts are not reduced at all (dotted line) and when 'school' and 'work' contacts are reduced by 100% (solid line).

3.4 Effect of surveillance on the contact-reducing NPIs required for local outbreak control

We considered whether or not low local outbreak probabilities can be achieved using limited contact-reducing NPIs in combination with other interventions. Specifically, the effects of

surveillance and isolation of infected individuals (through e.g. contact tracing) as well as reducing contacts in schools, workplaces and other locations, were assessed. While results are shown for scenario C in Fig 6, analogous results for scenarios A and B are presented in Supplementary Figs S3 and S6.

Initially, we considered the effect of increasing the rate at which symptomatic and/or nonsymptomatic infected individuals are detected and isolated as a result of surveillance, in the absence of contact-reducing NPIs (i.e. with no reduction in the number of contacts between individuals compared to the baseline case in Fig 2B) (Fig 6A,B). For symptomatic hosts, this represents an enhanced rate of isolation compared to the baseline rate of self-isolation already present in the model. Isolation of nonsymptomatic hosts was more effective at reducing the local outbreak probability than isolation of symptomatic hosts (Figs 6A,B), although of course this is more challenging to achieve [54]. However, if fast isolation of nonsymptomatic hosts could be achieved through efficient large-scale testing and contact tracing, the probability of local outbreaks could be reduced substantially through this measure alone.

We then demonstrated the effects of combining the isolation of infected hosts with reductions in the numbers of contacts between individuals. First, we increased the enhanced isolation rate of symptomatic individuals to $\rho_k = 1/2 \text{ days}^{-1}$. In the absence of other interventions, this reduced the local outbreak probability by 22.0% (Figure 6C). With this level of surveillance, the outbreak risk could be reduced below 0.01 with a reduction in ‘work’ and ‘other’ contacts of around 73% each, for example.

Finally, keeping the enhanced isolation rate of symptomatic individuals equal to $\rho_k = 1/2\ \text{days}^{-1}$, we increased the isolation rate of nonsymptomatic individuals to $\sigma_k = 1/7\ \text{days}^{-1}$. In this case, the local outbreak probability without contact-reducing NPIs fell by 59.4% compared to a situation without enhanced surveillance (Fig 6E), and the reductions in 'work' and 'other' contacts needed to bring the local outbreak probability below 0.01 were significantly smaller (Figure 6F). For example, if 'work' contacts can be reduced by 50%, then 'other' contacts only need to be reduced by 43%. This indicates that effective surveillance of both symptomatic and nonsymptomatic individuals can substantially lower the extent of contact-reducing NPIs that are required to achieve substantial reductions in local outbreak risks.

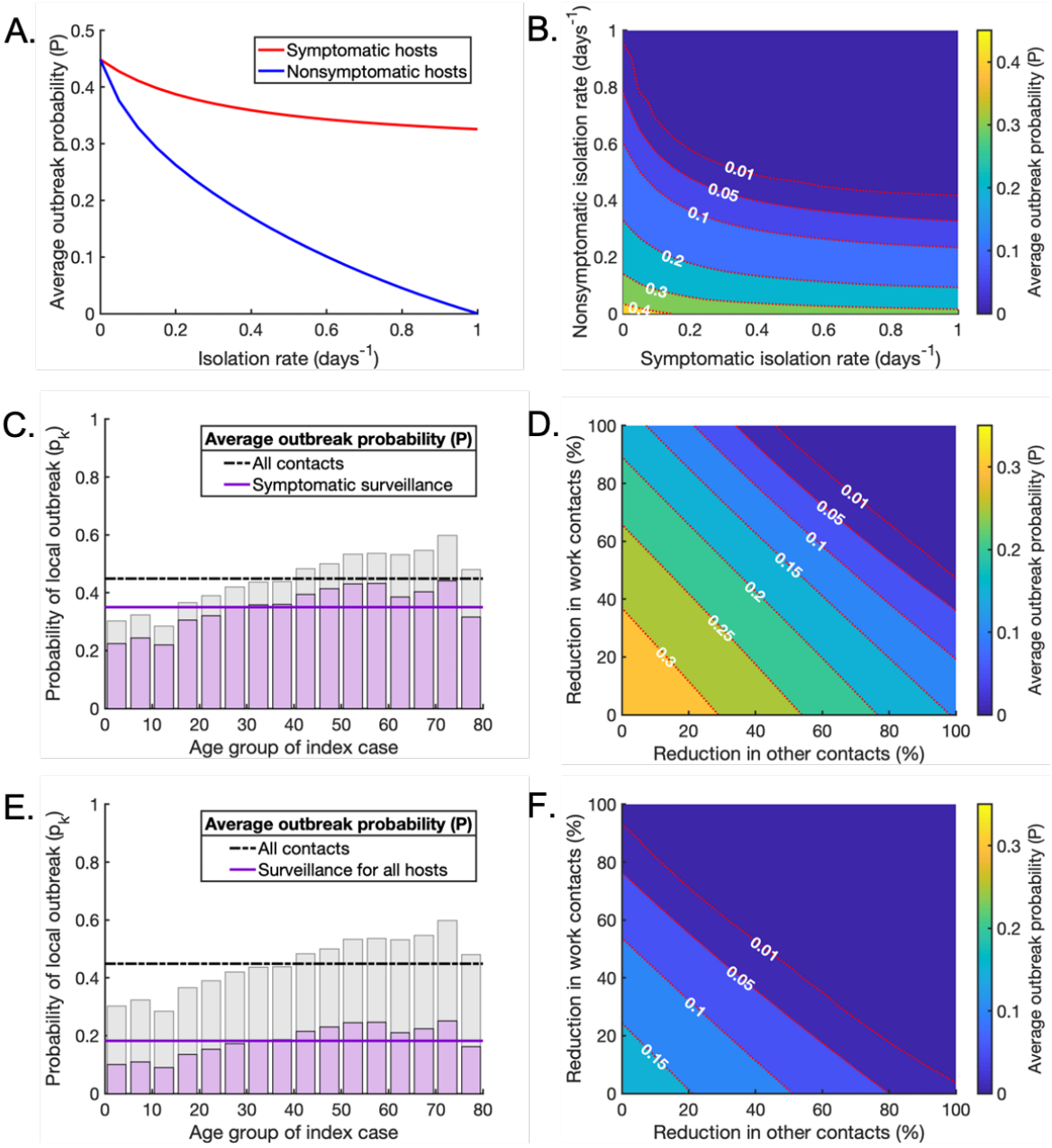

Fig 6. Surveillance as part of a mixed strategy to reduce the local outbreak probability. A. The effect of increasing the isolation rate of symptomatic (red line) or nonsymptomatic infected hosts (blue line) on the average probability of a local outbreak (P), in the absence of contact-reducing NPIs. The isolation rates ρ_k and σ_k are varied between 0 days^{-1} and 1 days^{-1}. B. The effect of simultaneously varying the isolation rate of symptomatic and nonsymptomatic hosts on the average probability of a local outbreak (P), again without contact-reducing NPIs. C. The age-dependent probability of a local outbreak

when the isolation rate of symptomatic individuals is $\rho_k = 1/2$ days^{-1}, without contact-reducing NPIs or surveillance of nonsymptomatic infected individuals (purple bars and solid line). Pale grey bars and black dash-dotted line represent the local outbreak probabilities without any contact-reducing NPIs or enhanced surveillance (as in Fig 3C). D. The effect of reducing 'work' and 'other' contacts when the isolation rate of symptomatic infected individuals is $\rho_k = 1/2$ days^{-1}, as in C, without surveillance of nonsymptomatic infected individuals. E,F. The analogous figures to C,D, with enhanced surveillance of both symptomatic and nonsymptomatic infected hosts ($\rho_k = 1/2$ days^{-1} and $\sigma_k = 1/7$ days^{-1}).

4. Discussion

During the COVID-19 pandemic, public health measures that reduce the numbers of contacts between individuals have been implemented in countries globally. These measures include school closures, workplace closures and population-wide social distancing policies. Contact-reducing NPIs have been shown to be effective at reducing SARS-CoV-2 transmission, and have also been used previously during influenza pandemics [5, 67-69]. However, long-term implementation of these measures has negative social, psychological and economic consequences [7, 11-15]. It is therefore important to assess the effectiveness of different contact-reducing NPIs at lowering transmission and preventing local outbreaks, in order to design effective targeted control strategies that avoid unnecessarily strict measures.

Here, we constructed a branching process model to estimate the risk of local outbreaks under different contact-reducing NPIs and different levels of surveillance for symptomatic and nonsymptomatic infected individuals. Unlike previous approaches for estimating outbreak risks using branching processes [50-55], we considered the effects of age-related heterogeneities affecting transmission for infected individuals of a wide range of ages, including age-dependent

525 variations in social mixing patterns, susceptibility to infection and clinical fraction. Using SARS-
526 CoV-2 as a case study, we demonstrated that the risk that an introduced case initiates a local
527 outbreak depends on these age-related factors and on the age of the introduced case (Fig 3), as
528 well as the age-structure of the local population.
529
530 We used our model to assess the effects of reducing the numbers of contacts that occur in school,
531 in the workplace and elsewhere. Of the three contact-reducing NPIs considered, removing
532 'school' contacts had the smallest effect on the probability of observing a local outbreak, even
533 when age-dependent variations in susceptibility and clinical fraction were ignored (Figs 4A,D,
534 Supplementary Figs S1A,D, and S4,A,D). This can be attributed to the fact that school closures
535 predominantly reduce contacts between individuals aged 5-19, who only account for
536 approximately 23% of the total population [57]. Additionally, these individuals tend to have
537 large numbers of contacts outside of the school environment (Figs 2E,F). Therefore, interrupting
538 within-school transmission may have only a limited effect on transmission in the wider
539 population, particularly when school-aged individuals are less susceptible to infection and more
540 likely to experience subclinical courses of infection. In contrast, reducing contacts that occur
541 outside schools or workplaces was the most effective intervention, significantly lowering the
542 outbreak risk across all age groups, and for those aged over 60 in particular (Figs 4C,D, and
543 Supplementary Figs S1C,D and S4C,D). This could explain the success of social distancing
544 strategies worldwide for reducing observed COVID-19 cases and deaths.
545
546 Mixed strategies combining reductions in 'school', 'work' and 'other' contacts led to greater
547 reductions in the outbreak probability than individual interventions (Figs 5A-C), but very large

548 reductions in all three types of contact were required to eliminate the risk of local outbreaks
549 entirely (Fig 5D). However, implementing effective surveillance to identify infected hosts led to
550 substantial reductions in the risk of local outbreaks even in the absence of other control measures
551 (Figs 6A,B). With an efficient surveillance strategy in place, significantly smaller reductions in
552 'work' and 'other' contacts were needed to render the outbreak probability negligible, even when
553 'school' contacts were not reduced at all (Figs 6C-F). This supports the use of surveillance that
554 targets both symptomatic and nonsymptomatic individuals, such as contact tracing and isolation
555 strategies or population-wide diagnostic testing, to prevent local outbreaks [54].
556
557 Although here we used SARS-CoV-2 as a case study, our model provides a framework for
558 estimating the risk of local outbreaks in age-structured populations that can be adapted for other
559 pathogens, provided sufficient data are available to parametrise the model appropriately. The
560 effects of age-structure on local outbreak risks may vary for pathogens with different
561 epidemiological characteristics. For influenza-A viruses, for example, susceptibility to infection
562 tends to decreases with age, whilst the risk of developing severe symptoms is greater both for the
563 elderly and for the very young [30, 70, 71]. This is in contrast to SARS-CoV-2, for which
564 children are more likely to experience subclinical courses of infection. In this study, we used age
565 demographic and contact data for the UK, but equivalent data for other countries are available
566 and can easily be substituted into our model to estimate outbreak risks elsewhere [16, 57].
567
568 One caveat of the results for SARS-CoV-2 presented here is that, although the epidemiological
569 parameters of our model were chosen to be consistent with reported literature estimates, there is
570 considerable variation between studies. In particular, the precise age-dependent variation in

susceptibility and clinical fraction remains unclear, and the relative infectiousness of asymptomatic, presymptomatic and symptomatic hosts has not been determined exactly. Furthermore, the inherent transmissibility of SARS-CoV-2 is now higher than in the initial stage of the pandemic, due to the appearance of new variants such as B.1.1.7. We therefore also conducted sensitivity analyses to explore the effects of varying the parameters of the model on our results (Supplementary Figs S1-12). In each case that we considered, our main conclusions were unchanged: the probability that an introduced case initiates a local outbreak depends on age-dependent factors affecting pathogen transmission and control, with widespread interventions and combinations of NPIs reducing the risk of local outbreaks most significantly.

An important limitation of our approach to modelling contact-reducing NPIs is that we made a standard assumption that 'school', 'work' and 'other' contacts are independent [26, 30, 46]. In other words, reducing the numbers of contacts in one location did not affect the numbers of contacts occurring in another. In reality, this is unlikely to be the case. For example, closing schools is also likely to affect workplace contacts, as adults may then work from home in order to fulfil childcare requirements. Additionally, the contact data that we used represent the number of unique contacts per day and do not include possible repeated contacts with the same person, which affect the risk of transmission between individuals. These assumptions could in principle be removed, if relevant data become available – for example, data describing the effects of school closures on numbers of contacts in other locations.

Despite these simplifications, our model provides a useful framework for estimating the risk of local outbreaks and the effects of NPIs. Different measures can be considered in combination in

the model to develop strategies for lowering local outbreak risks. Our results emphasise the importance of quantifying age-dependent factors that affect transmission dynamics, such as susceptibility to infection and the proportion of hosts who develop clinical symptoms, for individuals of different ages. As we have shown, it is crucial to take age-dependent factors into account when assessing outbreak risks and designing public health measures.

Declaration of interests

We declare no competing interests.

Authors' contributions

Conceptualisation: All authors. Methodology: FALR, RNT. Investigation: FALR, SS. Writing - original draft: FALR, RNT. Writing - review and editing: All authors. Supervision: RNT.

Data availability

All computer code used in this paper was written in MATLAB version R2019a, and is available at the following GitHub repository: https://github.com/francescalovellread/age-dependent-outbreak-risks.

Funding

FALR acknowledges funding from the Biotechnology and Biological Sciences Research Council (UKRI-BBSRC), grant number BB/M011224/1. SS was funded by a BBSRC Research

Experience Placement and a Rokos award for undergraduate research from Pembroke College Oxford.

References

[1] Perra, N. 2021, Online ahead of print. Non-pharmaceutical interventions during the COVID-19 pandemic: A review. *Phys. Rep.* (doi:10.1016/j.physrep.2021.02.001).

[2] Regmi, K. & Lwin, C.M. 2020 Impact of non-pharmaceutical interventions for reducing transmission of COVID-19: a systematic review and meta-analysis protocol. *BMJ Open* **10**, e041383. (doi:10.1136/bmjopen-2020-041383).

[3] Imai, N., Gaythorpe, K.A.M., Abbott, S., Bhatia, S., van Elsland, S., Prem, K., Liu, Y. & Ferguson, N.M. 2020 Adoption and impact of non-pharmaceutical interventions for COVID-19. *Wellcome Open Res* **5**, 59-59. (doi:10.12688/wellcomeopenres.15808.1).

[4] Thompson, R.N., Hollingsworth, T.D., Isham, V., Arribas-Bel, D., Ashby, B., Britton, T., Challenor, P., Chappell, L.H.K., Clapham, H., Cunniffe, N.J., et al. 2020 Key questions for modelling COVID-19 exit strategies. *Proc. R. Soc. Lond. B. Biol. Sci.* **287**, 20201405. (doi:10.1098/rspb.2020.1405).

[5] Hatchett, R.J., Mecher, C.E. & Lipsitch, M. 2007 Public health interventions and epidemic intensity during the 1918 influenza pandemic. *Proc. Natl. Acad. Sci. U. S. A.* **104**, 7582. (doi:10.1073/pnas.0610941104).

[6] Kirsch, T.D., Moseson, H., Massaquoi, M., Nyenswah, T.G., Goodermote, R., Rodriguez-Barraquer, I., Lessler, J., Cumings, D.A.T. & Peters, D.H. 2017 Impact of interventions and the incidence of ebola virus disease in Liberia—implications for future epidemics. *Health Policy Plan.* **32**, 205-214. (doi:10.1093/heapol/czw113).

638 [7] Berkman, B.E. 2008 Mitigating Pandemic Influenza: The Ethics of Implementing a School
639 Closure Policy. *J. Public Health Manag. Pract.* **14**, 372-378.
640 (doi:10.1097/01.PHH.0000324566.72533.0b).
641 [8] Moore, S., Hill, E.M., Tildesley, M.J., Dyson, L. & Keeling, M.J. 2021, Online ahead of
642 print. Vaccination and non-pharmaceutical interventions for COVID-19: a mathematical
643 modelling study. *Lancet Infect Dis*. (doi:10.1016/S1473-3099(21)00143-2).
644 [9] Spinelli, M.A., Glidden, D.V., Gennatas, E.D., Bielecki, M., Beyrer, C., Rutherford, G.,
645 Chambers, H., Goosby, E. & Gandhi, M. 2021, Online ahead of print. Importance of non-
646 pharmaceutical interventions in lowering the viral inoculum to reduce susceptibility to infection
647 by SARS-CoV-2 and potentially disease severity. *Lancet Infect Dis*. (doi:10.1016/S1473-
648 3099(20)30982-8).
649 [10] Thompson, R.N., Hill, E.M. & Gog, J.R. 2021, Online ahead of print/. SARS-CoV-2
650 incidence and vaccine escape. *Lancet Infect Dis*. (doi:10.1016/S1473-3099(21)00202-4).
651 [11] Donohue, J.M. & Miller, E. 2020 COVID-19 and School Closures. *JAMA* **324**, 845-847.
652 (doi:10.1001/jama.2020.13092).
653 [12] Silverman, M., Sibbald, R. & Stranges, S. 2020 Ethics of COVID-19-related school
654 closures. *Can. J. Public Health* **111**, 462-465. (doi:10.17269/s41997-020-00396-1).
655 [13] Sadique, M.Z., Adams, E.J. & Edmunds, W.J. 2008 Estimating the costs of school closure
656 for mitigating an influenza pandemic. *BMC Public Health* **8**, 135. (doi:10.1186/1471-2458-8-
657 135).
658 [14] Brooks, S.K., Webster, R.K., Smith, L.E., Woodland, L., Wessely, S., Greenberg, N. &
659 Rubin, G.J. 2020 The psychological impact of quarantine and how to reduce it: rapid review of
660 the evidence. *The Lancet* **395**, 912-920. (doi:10.1016/S0140-6736(20)30460-8).

661 [15] Loades, M.E., Chatburn, E., Higson-Sweeney, N., Reynolds, S., Shafran, R., Brigden, A.,
662 Linney, C., McManus, M.N., Borwick, C. & Crawley, E. 2020 Rapid Systematic Review: The
663 Impact of Social Isolation and Loneliness on the Mental Health of Children and Adolescents in
664 the Context of COVID-19. *J. Am. Acad. Child Adolesc. Psychiatry* **59**, 1218-1239.e1213.
665 (doi:10.1016/j.jaac.2020.05.009).
666 [16] Prem, K., Cook, A.R. & Jit, M. 2017 Projecting social contact matrices in 152 countries
667 using contact surveys and demographic data. *PLoS Comp. Biol.* **13**, e1005697.
668 (doi:10.1371/journal.pcbi.1005697).
669 [17] Mossong, J., Hens, N., Jit, M., Beutels, P., Auranen, K., Mikolajczyk, R., Massari, M.,
670 Salmaso, S., Tomba, G.S., Wallinga, J., et al. 2008 Social Contacts and Mixing Patterns Relevant
671 to the Spread of Infectious Diseases. *PLoS Med.* **5**, e74. (doi:10.1371/journal.pmed.0050074).
672 [18] Danon, L., Read, J.M., House, T.A., Vernon, M.C. & Keeling, M.J. 2013 Social encounter
673 networks: characterizing Great Britain. *Proc. R. Soc. Lond. B. Biol. Sci.* **280**, 20131037.
674 (doi:10.1098/rspb.2013.1037).
675 [19] Leung, K., Jit, M., Lau, E.H.Y. & Wu, J.T. 2017 Social contact patterns relevant to the
676 spread of respiratory infectious diseases in Hong Kong. *Sci. Rep.* **7**. (doi:10.1038/s41598-017-
677 08241-1).
678 [20] Béraud, G., Kazmercziak, S., Beutels, P., Levy-Bruhl, D., Lenne, X., Mielcarek, N.,
679 Yazdanpanah, Y., Boëlle, P.-Y., Hens, N. & Dervaux, B. 2015 The French Connection: The First
680 Large Population-Based Contact Survey in France Relevant for the Spread of Infectious
681 Diseases. *PLoS One* **10**, e0133203. (doi:10.1371/journal.pone.0133203).

682 [21] Ibuka, Y., Ohkusa, Y., Sugawara, T., Chapman, G.B., Yamin, D., Atkins, K.E., Taniguchi,
683 K., Okabe, N. & Galvani, A.P. 2016 Social contacts, vaccination decisions and influenza in
684 Japan. *J. Epidemiol. Community Health* **70**, 162-167. (doi:10.1136/jech-2015-205777).
685 [22] Read, J.M., Lessler, J., Riley, S., Wang, S., Tan, L.J., Kwok, K.O., Guan, Y., Jiang, C.Q. &
686 Cummings, D.A.T. 2014 Social mixing patterns in rural and urban areas of southern China. *Proc.*
687 *R. Soc. Lond. B. Biol. Sci.* **281**, 20140268. (doi:10.1098/rspb.2014.0268).
688 [23] Read, J.M., Edmunds, W.J., Riley, S., Lessler, J. & Cummings, D.A.T. 2012 Close
689 encounters of the infectious kind: methods to measure social mixing behaviour. *Epidemiol.*
690 *Infect.* **140**, 2117-2130. (doi:10.1017/S0950268812000842).
691 [24] Wallinga, J., Teunis, P. & Kretzschmar, M. 2006 Using Data on Social Contacts to Estimate
692 Age-specific Transmission Parameters for Respiratory-spread Infectious Agents. *Am. J.*
693 *Epidemiol.* **164**, 936-944. (doi:10.1093/aje/kwj317).
694 [25] Kucharski, A.J., Kwok, K.O., Wei, V.W.I., Cowling, B.J., Read, J.M., Lessler, J.,
695 Cummings, D.A. & Riley, S. 2014 The Contribution of Social Behaviour to the Transmission of
696 Influenza A in a Human Population. *PLoS Pathog.* **10**, e1004206.
697 (doi:10.1371/journal.ppat.1004206).
698 [26] Zhang, J., Litvinova, M., Liang, Y., Wang, Y., Wang, W., Zhao, S., Wu, Q., Merler, S.,
699 Viboud, C., Vespignani, A., et al. 2020 Changes in contact patterns shape the dynamics of the
700 COVID-19 outbreak in China. *Science* **368**, 1481-1486. (doi:10.1126/science.abb8001).
701 [27] Munro, A.P. & Faust, S.N. 2020 COVID-19 in children: current evidence and key
702 questions. *Curr. Opin. Infect. Dis.* **33**, 540-547. (doi:10.1097/QCO.0000000000000690).
703 [28] Viner, R.M., Mytton, O.T., Bonell, C., Melendez-Torres, G.J., Ward, J., Hudson, L.,
704 Waddington, C., Thomas, J., Russell, S., van der Klis, F., et al. 2021 Susceptibility to SARS-

705 CoV-2 Infection Among Children and Adolescents Compared With Adults: A Systematic
706 Review and Meta-analysis. *JAMA Pediatrics* **175**, 143-156.
707 (doi:10.1001/jamapediatrics.2020.4573).
708 [29] Goldstein, E., Lipsitch, M. & Cevik, M. 2020 On the effect of age on the transmission of
709 SARS-CoV-2 in households, schools and the community. *J. Infect. Dis.* **223**, 362-369.
710 (doi:10.1093/infdis/jiaa691).
711 [30] Davies, N.G., Klepac, P., Liu, Y., Prem, K., Jit, M., Pearson, C.A.B., Quilty, B.J.,
712 Kucharski, A.J., Gibbs, H., Clifford, S., et al. 2020 Age-dependent effects in the transmission
713 and control of COVID-19 epidemics. *Nat. Med.* **26**, 1205-1211. (doi:10.1038/s41591-020-0962-
714 9).
715 [31] Ludvigsson, J.F. 2020 Systematic review of COVID-19 in children shows milder cases and
716 a better prognosis than adults. *Acta paediatrica (Oslo, Norway : 1992)* **109**, 1088-1095.
717 (doi:10.1111/apa.15270).
718 [32] Dong, Y., Mo, X., Hu, Y., Qi, X., Jiang, F., Jiang, Z. & Tong, S. 2020 Epidemiology of
719 COVID-19 Among Children in China. *Pediatrics* **145**, e20200702. (doi:10.1542/peds.2020-
720 0702).
721 [33] Siebach, M.K., Piedimonte, G. & Ley, S.H. 2021, Online ahead of print. COVID-19 in
722 childhood: Transmission, clinical presentation, complications and risk factors. *Pediatr.*
723 *Pulmonol.* (doi:10.1002/ppul.25344).
724 [34] Mehta, N.S., Mytton, O.T., Mullins, E.W.S., Fowler, T.A., Falconer, C.L., Murphy, O.B.,
725 Langenberg, C., Jayatunga, W.J.P., Eddy, D.H. & Nguyen-Van-Tam, J.S. 2020 SARS-CoV-2
726 (COVID-19): What Do We Know About Children? A Systematic Review. *Clin. Infect. Dis.* **71**,
727 2469-2479. (doi:10.1093/cid/ciaa556).

728 [35] Han, M.S., Choi, E.H., Chang, S.H., Jin, B.-L., Lee, E.J., Kim, B.N., Kim, M.K., Doo, K.,
729 Seo, J.-H., Kim, Y.-J., et al. 2021 Clinical Characteristics and Viral RNA Detection in Children
730 With Coronavirus Disease 2019 in the Republic of Korea. *JAMA Pediatrics* **175**, 73-80.
731 (doi:10.1001/jamapediatrics.2020.3988).
732 [36] Pollock, A.M. & Lancaster, J. 2020 Asymptomatic transmission of covid-19. *BMJ* **371**,
733 m4851. (doi:10.1136/bmj.m4851).
734 [37] Buitrago-Garcia, D., Egli-Gany, D., Counotte, M.J., Hossmann, S., Imeri, H., Ipekci, A.M.,
735 Salanti, G. & Low, N. 2020 Occurrence and transmission potential of asymptomatic and
736 presymptomatic SARS-CoV-2 infections: A living systematic review and meta-analysis. *PLoS*
737 *Med.* **17**, e1003346. (doi:10.1371/journal.pmed.1003346).
738 [38] Byambasuren, O., Cardona, M., Bell, K., Clark, J., McLaws, M.-L. & Glasziou, P. 2020
739 Estimating the extent of asymptomatic COVID-19 and its potential for community transmission:
740 Systematic review and meta-analysis. *JAMMI* **5**, 223-234. (doi:10.3138/jammi-2020-0030).
741 [39] Koh, W.C., Naing, L., Chaw, L., Rosledzana, M.A., Alikhan, M.F., Jamaludin, S.A., Amin,
742 F., Omar, A., Shazli, A., Griffith, M., et al. 2020 What do we know about SARS-CoV-2
743 transmission? A systematic review and meta-analysis of the secondary attack rate and associated
744 risk factors. *PLoS One* **15**, e0240205. (doi:10.1371/journal.pone.0240205).
745 [40] Madewell, Z.J., Yang, Y., Longini, I.M., Jr., Halloran, M.E. & Dean, N.E. 2020 Household
746 Transmission of SARS-CoV-2: A Systematic Review and Meta-analysis. *JAMA Network Open*
747 **3**, e2031756-e2031756. (doi:10.1001/jamanetworkopen.2020.31756).
748 [41] Qiu, X., Nergiz, A.I., Maraolo, A.E., Bogoch, I.I., Low, N. & Cevik, M. 2021 Defining the
749 role of asymptomatic and pre-symptomatic SARS-CoV-2 transmission - a living systematic
750 review. *Clin. Microbiol. Infect.* **27**, 511-519. (doi:10.1016/j.cmi.2021.01.011).

751 [42] Pijls, B.G., Jolani, S., Atherley, A., Derckx, R.T., Dijkstra, J.I.R., Franssen, G.H.L.,
752 Hendriks, S., Richters, A., Venemans-Jellema, A., Zalpuri, S., et al. 2021 Demographic risk
753 factors for COVID-19 infection, severity, ICU admission and death: a meta-analysis of 59
754 studies. *BMJ Open* **11**, e044640. (doi:10.1136/bmjopen-2020-044640).
755 [43] Verity, R., Okell, L.C., Dorigatti, I., Winskill, P., Whittaker, C., Imai, N., Cuomo-
756 Dannenburg, G., Thompson, H., Walker, P.G.T., Fu, H., et al. 2020 Estimates of the severity of
757 coronavirus disease 2019: a model-based analysis. *Lancet Infect Dis* **20**, 669-677.
758 (doi:10.1016/S1473-3099(20)30243-7).
759 [44] Chen, T., Dai, Z., Mo, P., Li, X., Ma, Z., Song, S., Chen, X., Luo, M., Liang, K., Gao, S., et
760 al. 2020 Clinical Characteristics and Outcomes of Older Patients with Coronavirus Disease 2019
761 (COVID-19) in Wuhan, China: A Single-Centered, Retrospective Study. *J. Gerontol. A Biolo.*
762 *Sci. Med. Sci.* **75**, 1788-1795. (doi:10.1093/gerona/glaa089).
763 [45] Prem, K., Liu, Y., Russell, T.W., Kucharski, A.J., Eggo, R.M., Davies, N., Flasche, S.,
764 Clifford, S., Pearson, C.A.B., Munday, J.D., et al. 2020 The effect of control strategies to reduce
765 social mixing on outcomes of the COVID-19 epidemic in Wuhan, China: a modelling study.
766 *Lancet Public Health* **5**, e261-e270. (doi:10.1016/S2468-2667(20)30073-6).
767 [46] Davies, N.G., Kucharski, A.J., Eggo, R.M., Gimma, A., Edmunds, W.J. & Centre for the
768 Mathematical Modelling of Infectious Diseases COVID-19 working group. 2020 Effects of non-
769 pharmaceutical interventions on COVID-19 cases, deaths, and demand for hospital services in
770 the UK: a modelling study. *Lancet Public Health* **5**, e375-e385. (doi:10.1016/S2468-
771 2667(20)30133-X).

[47] Liu, T., Gong, D., Xiao, J., Hu, J., He, G., Rong, Z. & Ma, W. 2020 Cluster infections play important roles in the rapid evolution of COVID-19 transmission: A systematic review. *Int. J. Infect. Dis.* **99**, 374-380. (doi:10.1016/j.ijid.2020.07.073).

[48] Leclerc, Q., Fuller, N., Knight, L., null, n., Funk, S. & Knight, G. 2020 What settings have been linked to SARS-CoV-2 transmission clusters? [version 2; peer review: 2 approved]. *Wellcome Open Res* **5**. (doi:10.12688/wellcomeopenres.15889.2).

[49] Rossman, H., Keshet, A., Shilo, S., Gavrieli, A., Bauman, T., Cohen, O., Shelly, E., Balicer, R., Geiger, B., Dor, Y., et al. 2020 A framework for identifying regional outbreak and spread of COVID-19 from one-minute population-wide surveys. *Nat. Med.* **26**, 634-638. (doi:10.1038/s41591-020-0857-9).

[50] Althaus, C.L., Low, N., Musa, E.O., Shuaib, F. & Gsteiger, S. 2015 Ebola virus disease outbreak in Nigeria: Transmission dynamics and rapid control. *Epidemics* **11**, 80-84. (doi:10.1016/j.epidem.2015.03.001).

[51] Thompson, R.N., Jalava, K. & Obolski, U. 2019 Sustained transmission of Ebola in new locations: more likely than previously thought. *Lancet Infect Dis* **19**, 1058-1059. (doi:10.1016/S1473-3099(19)30483-9).

[52] Thompson, R.N. 2020 Novel Coronavirus Outbreak in Wuhan, China, 2020: Intense Surveillance Is Vital for Preventing Sustained Transmission in New Locations. *J. Clin. Med.* **9**, 498. (doi:10.3390/jcm9020498).

[53] Hellewell, J., Abbott, S., Gimma, A., Bosse, N.I., Jarvis, C.I., Russell, T.W., Munday, J.D., Kucharski, A.J., Edmunds, W.J., Sun, F., et al. 2020 Feasibility of controlling COVID-19 outbreaks by isolation of cases and contacts. *Lancet Glob. Health* **8**, e488-e496. (doi:10.1016/S2214-109X(20)30074-7).

[54] Lovell-Read, F.A., Funk, S., Obolski, U., Donnelly, C.A. & Thompson, R.N. In press. Interventions targeting nonsymptomatic cases can be important to prevent local outbreaks: SARS-CoV-2 as a case-study. *J. R. Soc. Interface*. (doi:10.1101/2020.11.06.20226969).

[55] Nishiura, H., Cook, A.R. & Cowling, B.J. 2011 Assortativity and the Probability of Epidemic Extinction: A Case Study of Pandemic Influenza A (H1N1-2009). *Interdiscip. Perspect. Infect. Dis.* **2011**, 194507. (doi:10.1155/2011/194507).

[56] Ferretti, L., Wymant, C., Kendall, M., Zhao, L., Nurtay, A., Abeler-Dorner, L., Parker, M., Bonsall, D. & Fraser, C. 2020 Quantifying SARS-CoV-2 transmission suggests epidemic control with digital contact tracing. *Science* **368**, eabb6936. (doi:10.1126/science.abb6936).

[57] United Nations, Department of Economic and Social Affairs, Population Division. 2019 World Population Prospects 2019, Online Edition, Rev. 1. *Available at:* *https://population.un.org/wpp/Download/Standard/Population/*.

[58] Wei, W.E., Li, Z., Chiew, C.J., Yong, S.E., Toh, M.P. & Lee, V.J. 2020 Presymptomatic Transmission of SARS-CoV-2 — Singapore, January 23–March 16, 2020. *Morb. Mortal. Weekly Rep.* **69**, 411-415. (doi:10.15585/mmwr.mm6914e1external icon).

[59] Arons, M.M., Hatfield, K.M., Reddy, S.C., Kimball, A., James, A., Jacobs, J.R., Taylor, J., Spicer, K., Bardossy, A.C., Oakley, L.P., et al. 2020 Presymptomatic SARS-CoV-2 Infections and Transmission in a Skilled Nursing Facility. *N. Engl. J. Med.* **382**, 2081-2090. (doi:10.1056/NEJMoa2008457).

[60] Bullard, J., Dust, K., Funk, D., Strong, J.E., Alexander, D., Garnett, L., Boodman, C., Bello, A., Hedley, A., Schiffman, Z., et al. 2020 Predicting Infectious Severe Acute Respiratory Syndrome Coronavirus 2 From Diagnostic Samples. *Clin. Infect. Dis.* **71**, 2663-2666. (doi:10.1093/cid/ciaa638).

818 [61] Wolfel, R., Corman, V.M., Guggemos, W., Seilmaier, M., Zange, S., Muller, M.A.,
819 Niemeyer, D., Jones, T.C., Vollmar, P., Rothe, C., et al. 2020 Virological assessment of
820 hospitalized patients with COVID-2019. *Nature* **581**, 465-469. (doi:10.1038/s41586-020-2196-
821 x).
822 [62] Lai, C.-C., Shih, T.-P., Ko, W.-C., Tang, H.-J. & Hsueh, P.-R. 2020 Severe acute respiratory
823 syndrome coronavirus 2 (SARS-CoV-2) and coronavirus disease-2019 (COVID-19): The
824 epidemic and the challenges. *Int. J. Antimicrob. Agents* **55**, 105924.
825 (doi:10.1016/j.ijantimicag.2020.105924).
826 [63] Liu, Y., Gayle, A.A., Wilder-Smith, A. & Rocklov, J. 2020 The reproductive number of
827 COVID-19 is higher compared to SARS coronavirus. *J. Travel Med.* **27**, taaa021.
828 (doi:10.1093/jtm/taaa021).
829 [64] Zhai, P., Ding, Y., Wu, X., Long, J., Zhong, Y. & Li, Y. 2020 The epidemiology, diagnosis
830 and treatment of COVID-19. *Int. J. Antimicrob. Agents* **55**, 105955-105955.
831 (doi:10.1016/j.ijantimicag.2020.105955).
832 [65] Zhao, S., Lin, Q., Ran, J., Musa, S.S., Yang, G., Wang, W., Lou, Y., Gao, D., Yang, L., He,
833 D., et al. 2020 Preliminary estimation of the basic reproduction number of novel coronavirus
834 (2019-nCoV) in China, from 2019 to 2020: A data-driven analysis in the early phase of the
835 outbreak. *Int. J. Infect. Dis.* **92**, 214-217. (doi:10.1016/j.ijid.2020.01.050).
836 [66] Norris, J.R. 1997 *Markov Chains (Cambridge Series in Statistical and Probabilistic*
837 *Mathematics)*. Cambridge, Cambridge University Press.
838 [67] Huang, Q.S., Wood, T., Jelley, L., Jennings, T., Jefferies, S., Daniells, K., Nesdale, A.,
839 Dowell, T., Turner, N., Campbell-Stokes, P., et al. 2021 Impact of the COVID-19

840 nonpharmaceutical interventions on influenza and other respiratory viral infections in New
841 Zealand. *Nat. Commun.* **12**, 1001. (doi:10.1038/s41467-021-21157-9).
842 [68] Flaxman, S., Mishra, S., Gandy, A., Unwin, H.J.T., Mellan, T.A., Coupland, H., Whittaker,
843 C., Zhu, H., Berah, T., Eaton, J.W., et al. 2020 Estimating the effects of non-pharmaceutical
844 interventions on COVID-19 in Europe. *Nature* **584**, 257-261. (doi:10.1038/s41586-020-2405-7).
845 [69] Borse, R.H., Behravesh, C.B., Dumanovsky, T., Zucker, J.R., Swerdlow, D., Edelson, P.,
846 Choe-Castillo, J. & Meltzer, M.I. 2011 Closing Schools in Response to the 2009 Pandemic
847 Influenza A H1N1 Virus in New York City: Economic Impact on Households. *Clin. Infect. Dis.*
848 **52**, S168-S172. (doi:10.1093/cid/ciq033).
849 [70] Greer, A.L., Tuite, A. & Fisman, D.N. 2010 Age, influenza pandemics and disease
850 dynamics. *Epidemiol. Infect.* **138**, 1542-1549. (doi:10.1017/S0950268810000579).
851 [71] Clohisey, S. & Baillie, J.K. 2019 Host susceptibility to severe influenza A virus infection.
852 *Crit. Care* **23**, 303. (doi:10.1186/s13054-019-2566-7).

Supplementary Figures

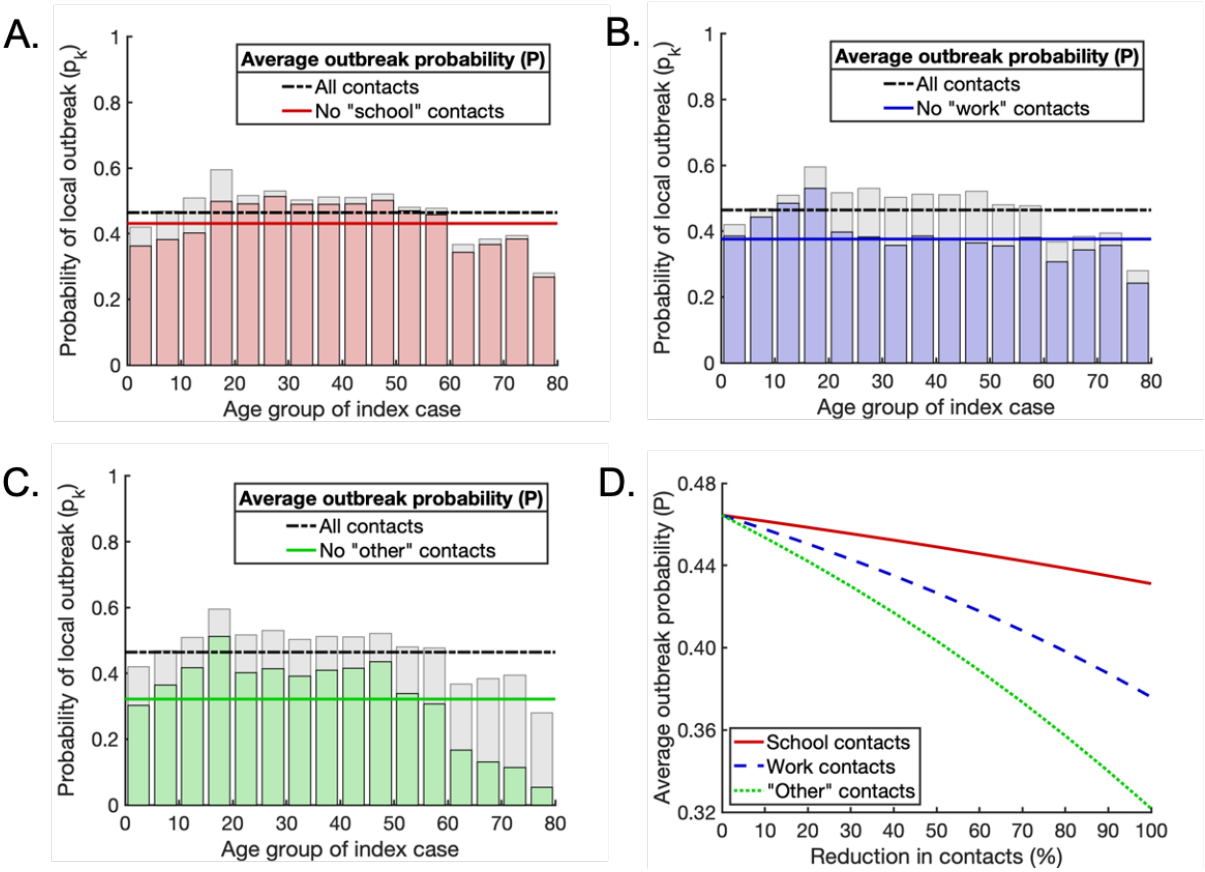

Fig S1. Scenario A: The effects of interventions that reduce contacts between individuals on the probability of a local outbreak. For scenario A, susceptibility to infection and the proportion of hosts who experience a fully asymptomatic course of infection are independent of age. A. The effect of removing all 'school' contacts on the probability of a local outbreak. Pale grey bars and black dash-dotted line represent the local outbreak probabilities without any contacts removed (as in Fig 3A). Red bars and the solid red line represent the local outbreak probabilities and their weighted average when 'school' contacts are removed. B. The analogous figure to A, but with all 'work' contacts removed. C. The analogous figure to A, but with all 'other' contacts removed. D. Partial reductions in 'school', 'work' and 'other' contacts, and the resulting reductions in average local outbreak probability (solid red, dashed blue and dotted green lines respectively).

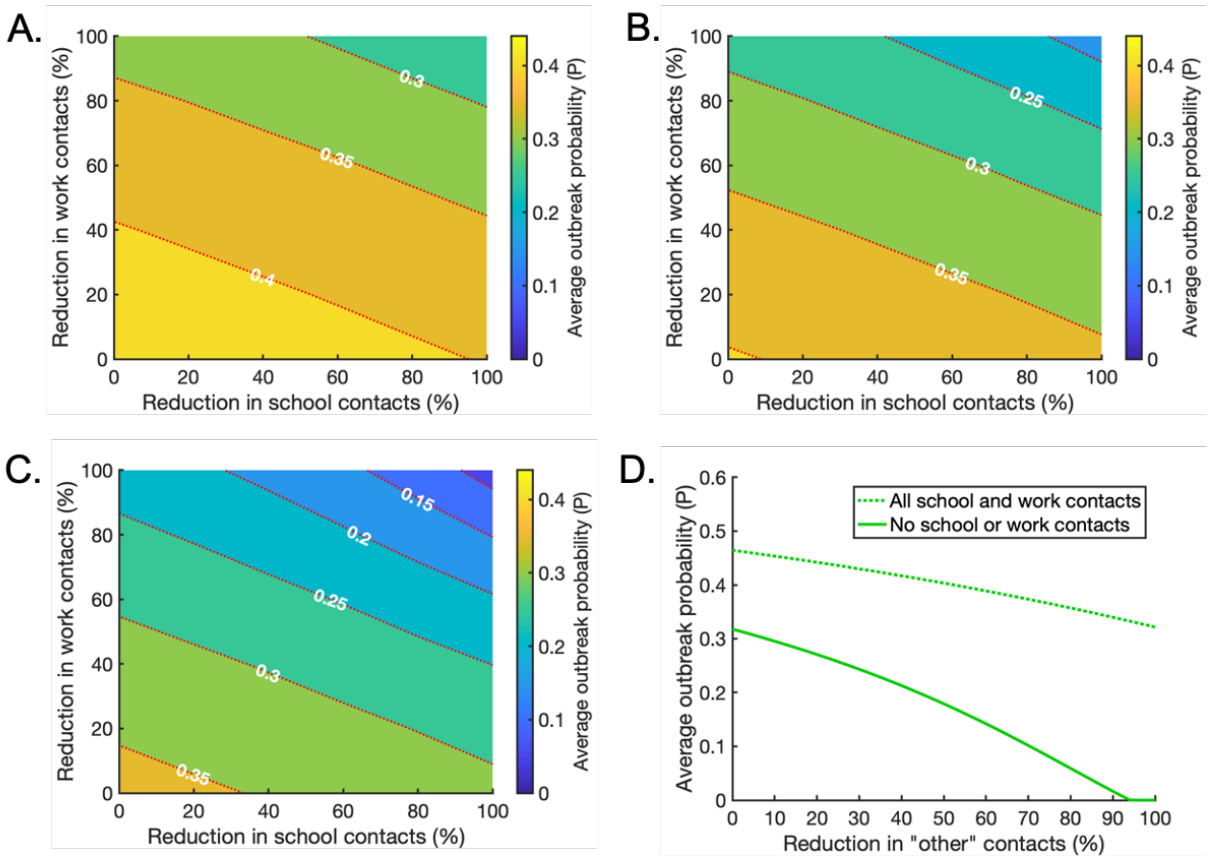

Fig S2. Scenario A: The effects of intervention strategies that combine reductions in 'school', 'work' and 'other' contacts. For scenario A, susceptibility to infection and the proportion of hosts who experience a fully asymptomatic course of infection are independent of age. A. The effect of reducing 'school' and 'work' contacts on the weighted average probability of a local outbreak (*P*), when 'other' contacts are reduced by 25% across all age groups. Red dotted lines indicate contours along which the local outbreak probability is constant. B. The analogous figure to A, but with a 50% reduction in 'other' contacts. C. The analogous figure to A, but with a 75% reduction in 'other' contacts. D. The effect of reducing 'other' contacts on the average local outbreak probability when 'school' and 'work' contacts are not reduced at all (dotted line) and when 'school' and 'work' contacts are reduced by 100% (solid line).

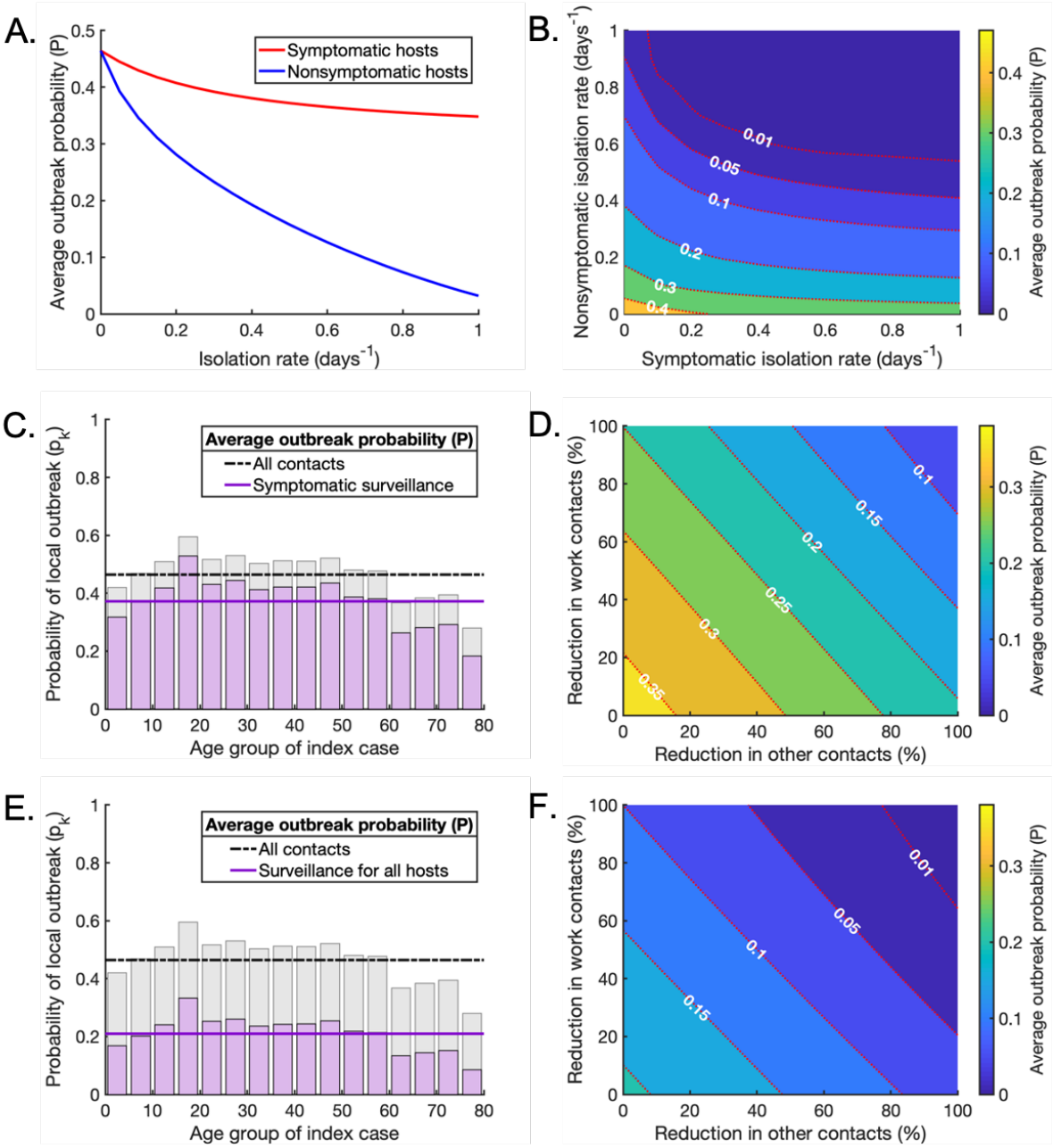

Fig S3. Scenario A: Surveillance as part of a mixed strategy to reduce the local outbreak probability. For scenario A, susceptibility to infection and the proportion of hosts who experience a fully asymptomatic course of infection are independent of age. A. The effect of increasing the isolation rate of symptomatic (red line) or nonsymptomatic infected hosts (blue line) on the average probability of a local outbreak (P), in the absence of contact-reducing NPIs. The isolation rates ρ_k and σ_k are varied between 0 days^{-1} and 1 days^{-1}. B. The effect of simultaneously varying the isolation rate of symptomatic and nonsymptomatic

hosts on the average probability of a local outbreak (P), again without contact-reducing NPIs. C. The age-dependent probability of a local outbreak when the isolation rate for symptomatic individuals is $\rho_k = 1/2\ \text{days}^{-1}$, without contact-reducing NPIs or surveillance of nonsymptomatic infected individuals (purple bars and solid line). Pale grey bars and black dash-dotted line represent the local outbreak probabilities without any contact-reducing NPIs or enhanced surveillance (as in Fig 3A). D. The effect of reducing 'work' and 'other' contacts when the isolation rate of symptomatic individuals is $\rho_k = 1/2\ \text{days}^{-1}$, as in C, without surveillance of nonsymptomatic infected individuals. E,F. The analogous figures to C,D, with enhanced surveillance of both symptomatic and nonsymptomatic infected hosts ($\rho_k = 1/2\ \text{days}^{-1}$ and $\sigma_k = 1/7\ \text{days}^{-1}$).

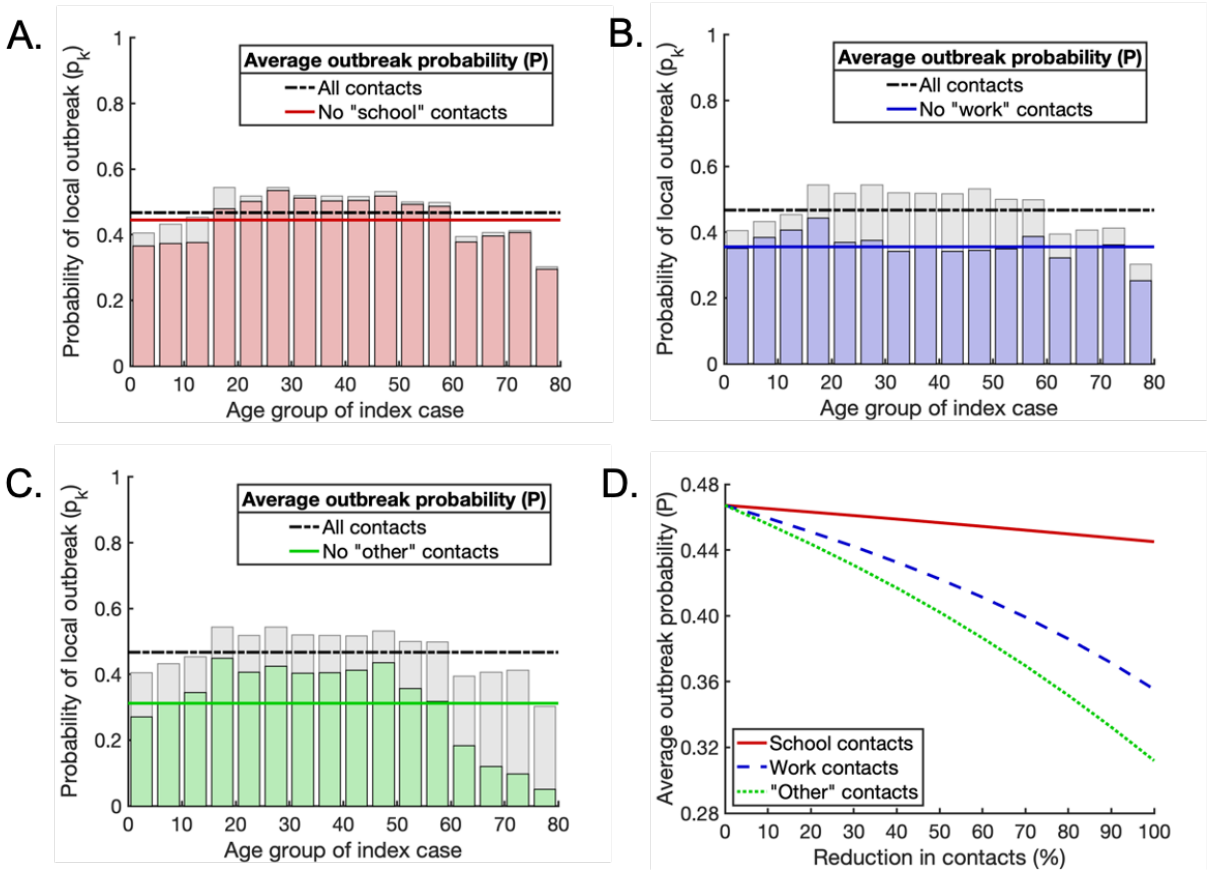

Fig S4. Scenario B: The effects of interventions that reduce contacts between individuals on the probability of a local outbreak. For scenario B, susceptibility to infection varies with age but the proportion of hosts who experience a fully asymptomatic course of infection are independent of age. A. The

effect of removing all ‘school’ contacts on the probability of a local outbreak. Pale grey bars and black dash-dotted line represent the local outbreak probabilities without any contacts removed (as in Fig 3B). Red bars and the solid red line represent the local outbreak probabilities and their weighted average when ‘school’ contacts are removed. B. The analogous figure to A, but with all ‘work’ contacts removed. C. The analogous figure to A, but with all ‘other’ contacts removed. D. Partial reductions in ‘school’, ‘work’ and ‘other’ contacts, and the resulting reductions in average local outbreak probability (solid red, dashed blue and dotted green lines respectively).

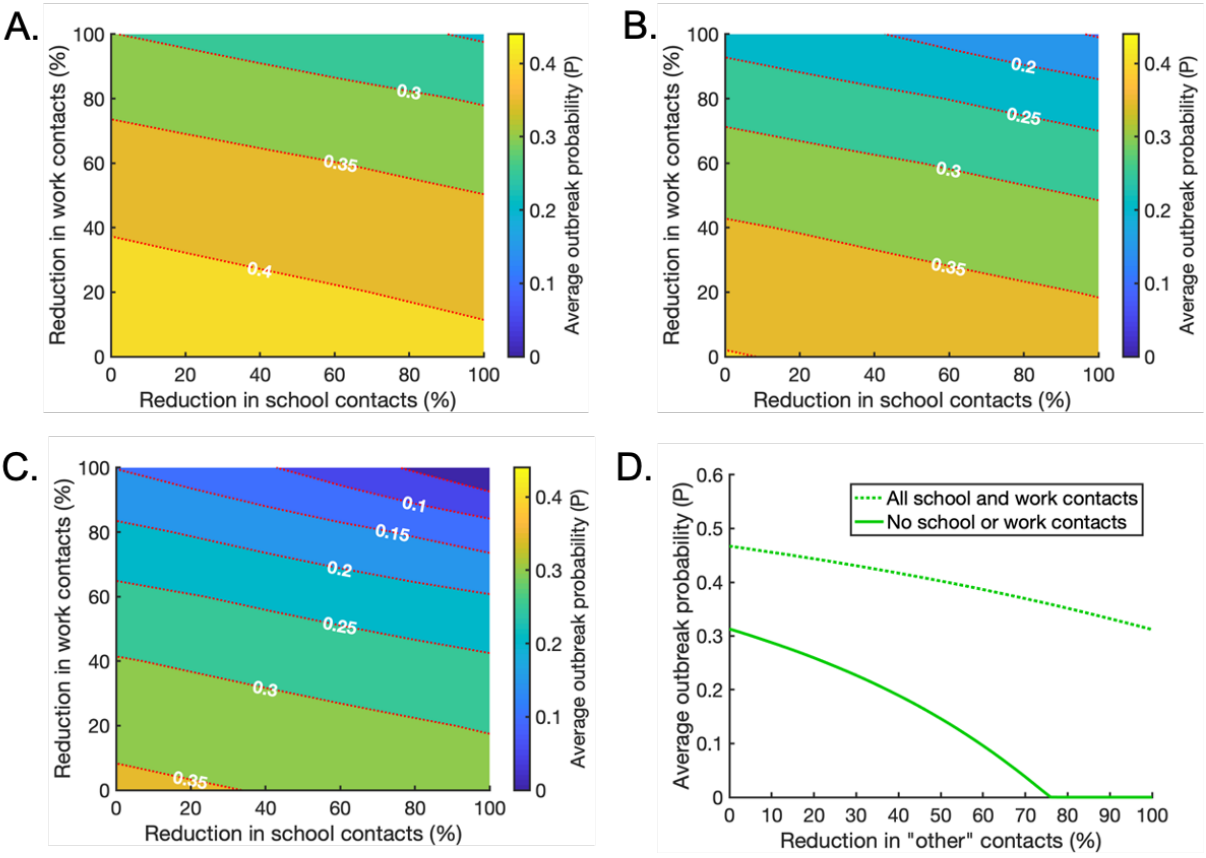

Fig S5. Scenario B: The effects of intervention strategies that combine reductions in ‘school’, ‘work’ and ‘other’ contacts. For scenario B, susceptibility to infection varies with age but the proportion of hosts who experience a fully asymptomatic course of infection are independent of age. A. The effect of reducing ‘school’ and ‘work’ contacts on the weighted average probability of a local outbreak (*P*), when ‘other’ contacts are reduced by 25% across all age groups. Red dotted lines indicate contours along which the local

outbreak probability is constant. B. The analogous figure to A, but with a 50% reduction in ‘other’ contacts. C. The analogous figure to A, but with a 75% reduction in ‘other’ contacts. D. The effect of reducing ‘other’ contacts on the average local outbreak probability when ‘school’ and ‘work’ contacts are not reduced at all (dotted line) and when ‘school’ and ‘work’ contacts are reduced by 100% (solid line).

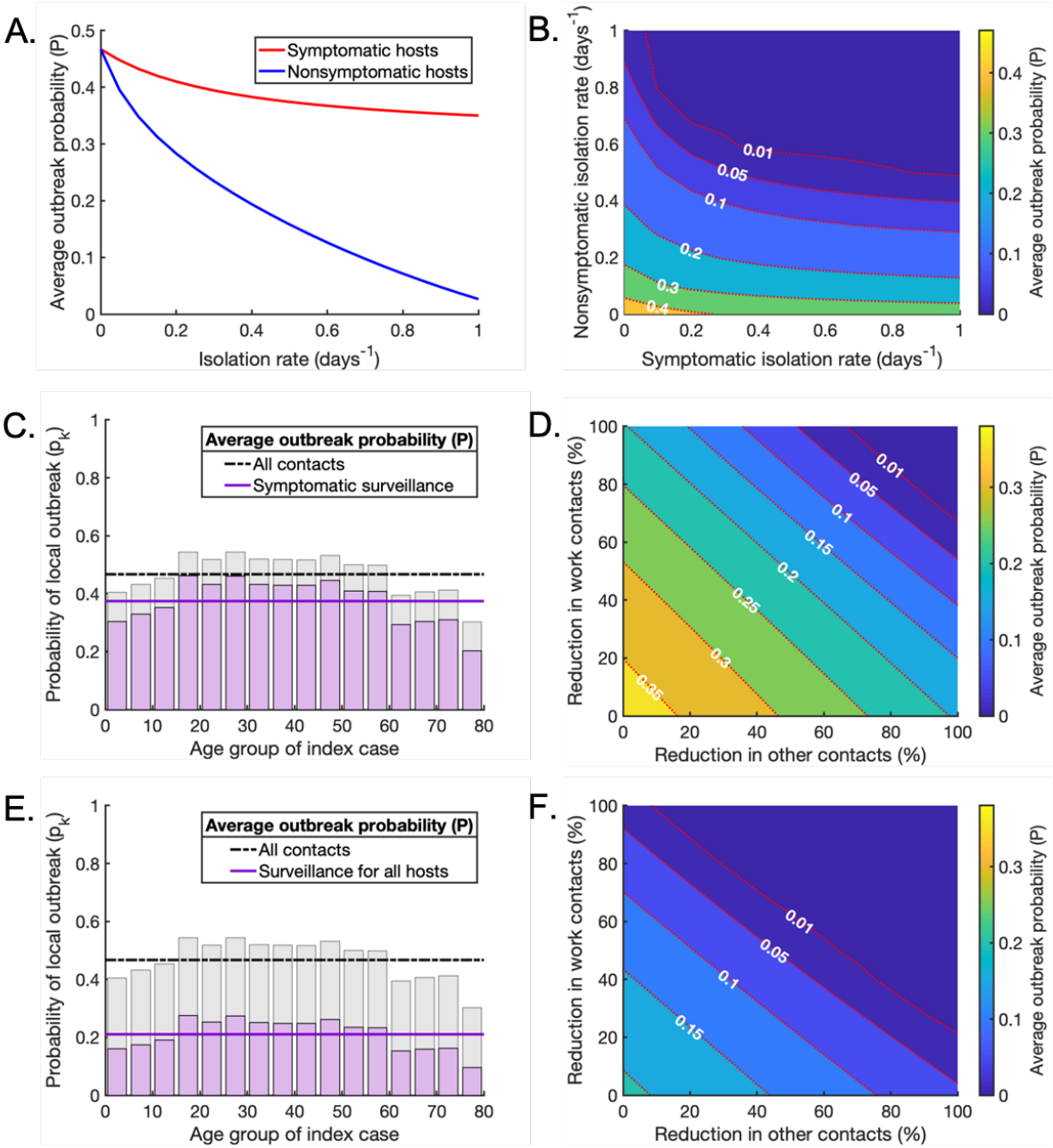

Fig S6. Scenario B: Surveillance as part of a mixed strategy to reduce the local outbreak probability. For scenario B, susceptibility to infection varies with age but the proportion of hosts who experience a fully asymptomatic course of infection are independent of age. A. The effect of increasing the isolation rate of symptomatic (red line) or nonsymptomatic infected hosts (blue line) on the average probability of a local outbreak (P), in the absence of contact-reducing NPIs. The isolation rates ρ_k and σ_k are varied between $0\ \text{days}^{-1}$ and $1\ \text{days}^{-1}$. B. The effect of simultaneously varying the isolation rate of symptomatic and nonsymptomatic hosts on the average probability of a local outbreak (P), again without contact-reducing NPIs. C. The age-dependent probability of a local outbreak when the isolation rate of symptomatic individuals is $\rho_k = 1/2\ \text{days}^{-1}$, without contact-reducing NPIs or surveillance of nonsymptomatic infected individuals (purple bars and solid line). Pale grey bars and black dash-dotted line represent the local outbreak probabilities without any contact reducing NPIs or enhanced surveillance (as in Fig 3B). D. The effect of reducing 'work' and 'other' contacts when the isolation rate of symptomatic individuals is $\rho_k = 1/2\ \text{days}^{-1}$, as in C, without surveillance of nonsymptomatic infected individuals. E,F. The analogous figures to C,D, with enhanced surveillance of both symptomatic and nonsymptomatic infected hosts ($\rho_k = 1/2\ \text{days}^{-1}$ and $\sigma_k = 1/7\ \text{days}^{-1}$).

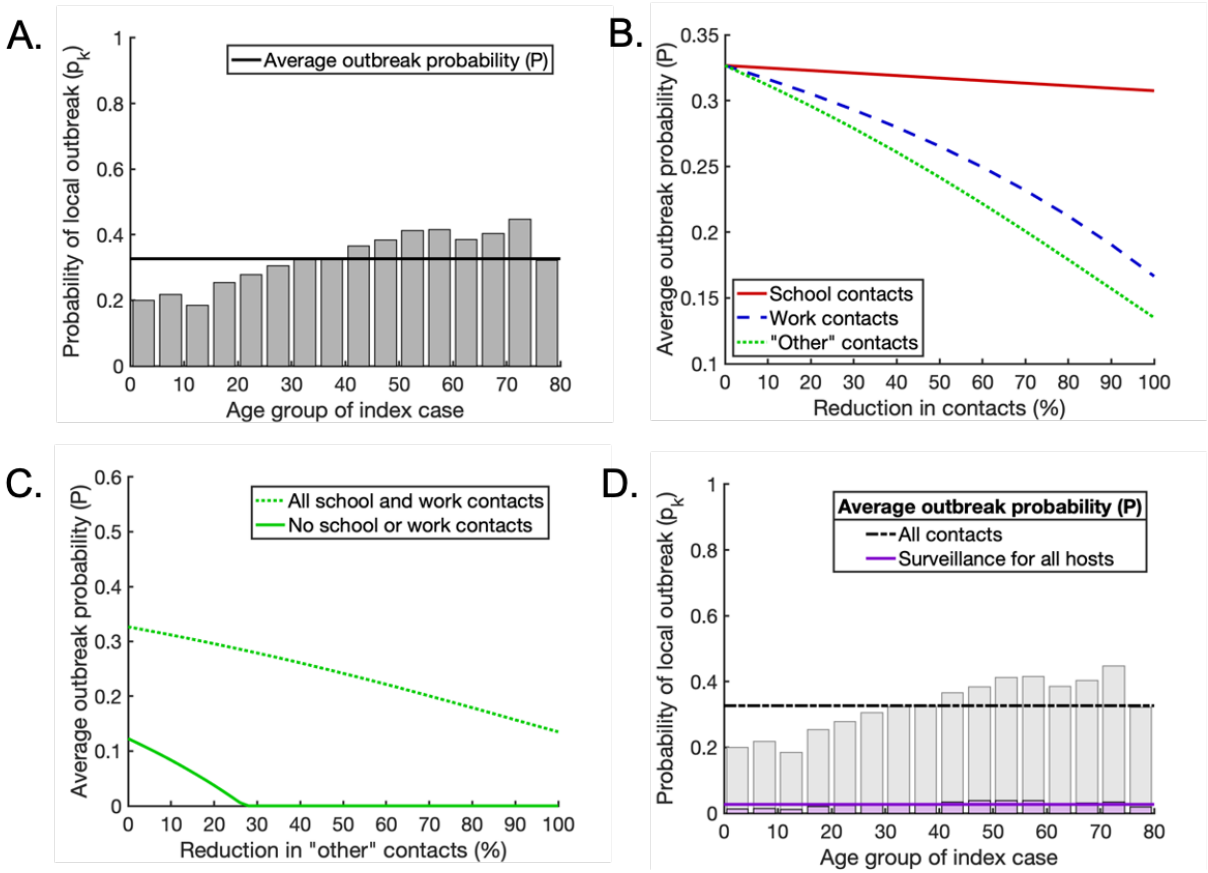

Fig S7. Scenario C: The effect of reducing the basic reproduction number from $R_0 = 3$ (baseline value) to $R_0 = 2$. For scenario C, both susceptibility to infection and the proportion of hosts who experience a fully asymptomatic course of infection vary with age. A. Analogous to Fig 3C in the main text: the probability that a single infected individual in any given age group triggers a local outbreak (grey bars) and the weighted average local outbreak probability P (black horizontal line). B. Analogous to Fig 4D in the main text: partial reductions in 'school', 'work' and 'other' contacts, and the resulting reductions in the average local outbreak probability P (solid red, dashed blue and dotted green lines respectively). C. Analogous to Fig 5D in the main text: the effect of reducing 'other' contacts on the average local outbreak probability when 'school' and 'work' contacts are not reduced at all (dotted line) and when 'school' and 'work' contacts are reduced by 100% (solid line). D. Analogous to Fig 6E in the main text: the age-dependent probability of a local outbreak with enhanced surveillance of both symptomatic and nonsymptomatic infected hosts ($\rho_k = 1/2$ days^{-1} and $\sigma_k = 1/7$ days^{-1}), without contact-reducing NPIs

(purple bars and solid line). Pale grey bars and black dash-dotted line represent the local outbreak probabilities without any contact-reducing NPIs or enhanced surveillance (as in Fig S7A).

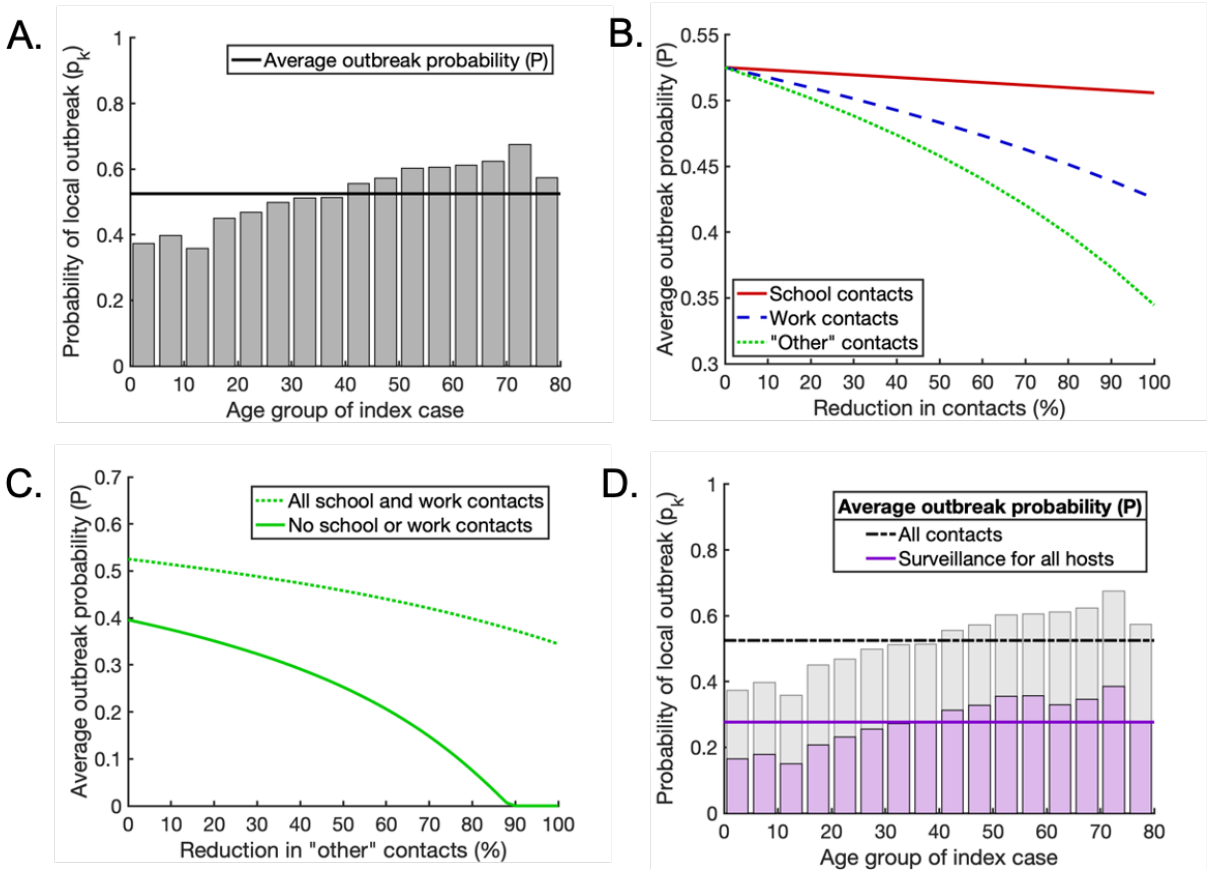

Fig S8. Scenario C: The effect of increasing the basic reproduction number from $R_0 = 3$ (baseline value) to $R_0 = 4$. For scenario C, both susceptibility to infection and the proportion of hosts who experience a fully asymptomatic course of infection vary with age. A. Analogous to Fig 3C in the main text: the probability that a single infected individual in any given age group triggers a local outbreak (grey bars) and the weighted average local outbreak probability *P* (black horizontal line). B. Analogous to Fig 4D in the main text: partial reductions in 'school', 'work' and 'other' contacts, and the resulting reductions in the average local outbreak probability *P* (solid red, dashed blue and dotted green lines respectively). C. Analogous to Fig 5D in the main text: the effect of reducing 'other' contacts on the average local outbreak probability when 'school' and 'work' contacts are not reduced at all (dotted line) and when 'school' and

'work' contacts are reduced by 100% (solid line). D. Analogous to Fig 6E in the main text: the age-dependent probability of a local outbreak with enhanced surveillance of both symptomatic and nonsymptomatic infected hosts ($\rho_k = 1/2$ days^{-1} and $\sigma_k = 1/7$ days^{-1}), without contact-reducing NPIs (purple bars and solid line). Pale grey bars and black dash-dotted line represent the local outbreak probabilities without any contact-reducing NPIs or enhanced surveillance (as in Fig S8A).

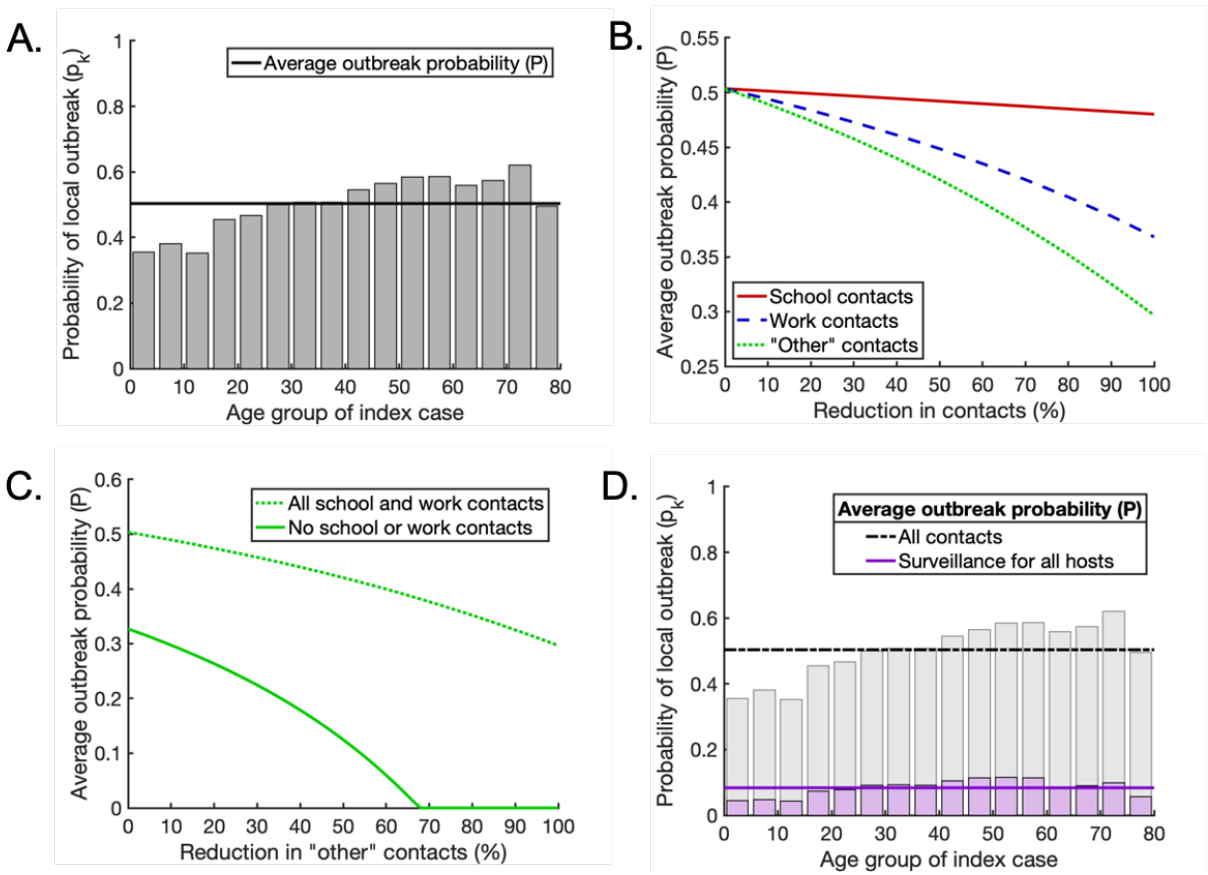

Fig S9. Scenario C: The effect of reducing the proportion of infections that arise from presymptomatic hosts from $K_p = 0.489$ (baseline value) to $K_p = 0.25$. The proportions of infections arising from symptomatic and asymptomatic hosts are adjusted so that they remain in the same ratio as in the baseline case. For scenario C, both susceptibility to infection and the proportion of hosts who experience a fully asymptomatic course of infection vary with age. A. Analogous to Fig 3C in the main

text: the probability that a single infected individual in any given age group triggers a local outbreak (grey bars) and the weighted average local outbreak probability P (black horizontal line). B. Analogous to Fig 4D in the main text: partial reductions in 'school', 'work' and 'other' contacts, and the resulting reductions in the average local outbreak probability P (solid red, dashed blue and dotted green lines respectively). C. Analogous to Fig 5D in the main text: the effect of reducing 'other' contacts on the average local outbreak probability when 'school' and 'work' contacts are not reduced at all (dotted line) and when 'school' and 'work' contacts are reduced by 100% (solid line). D. Analogous to Fig 6E in the main text: the age-dependent probability of a local outbreak with enhanced surveillance of both symptomatic and nonsymptomatic infected hosts ($\rho_k = 1/2$ days^{-1} and $\sigma_k = 1/7$ days^{-1}), without contact-reducing NPIs (purple bars and solid line). Pale grey bars and black dash-dotted line represent the local outbreak probabilities without any contact-reducing NPIs or enhanced surveillance (as in Fig S9A).

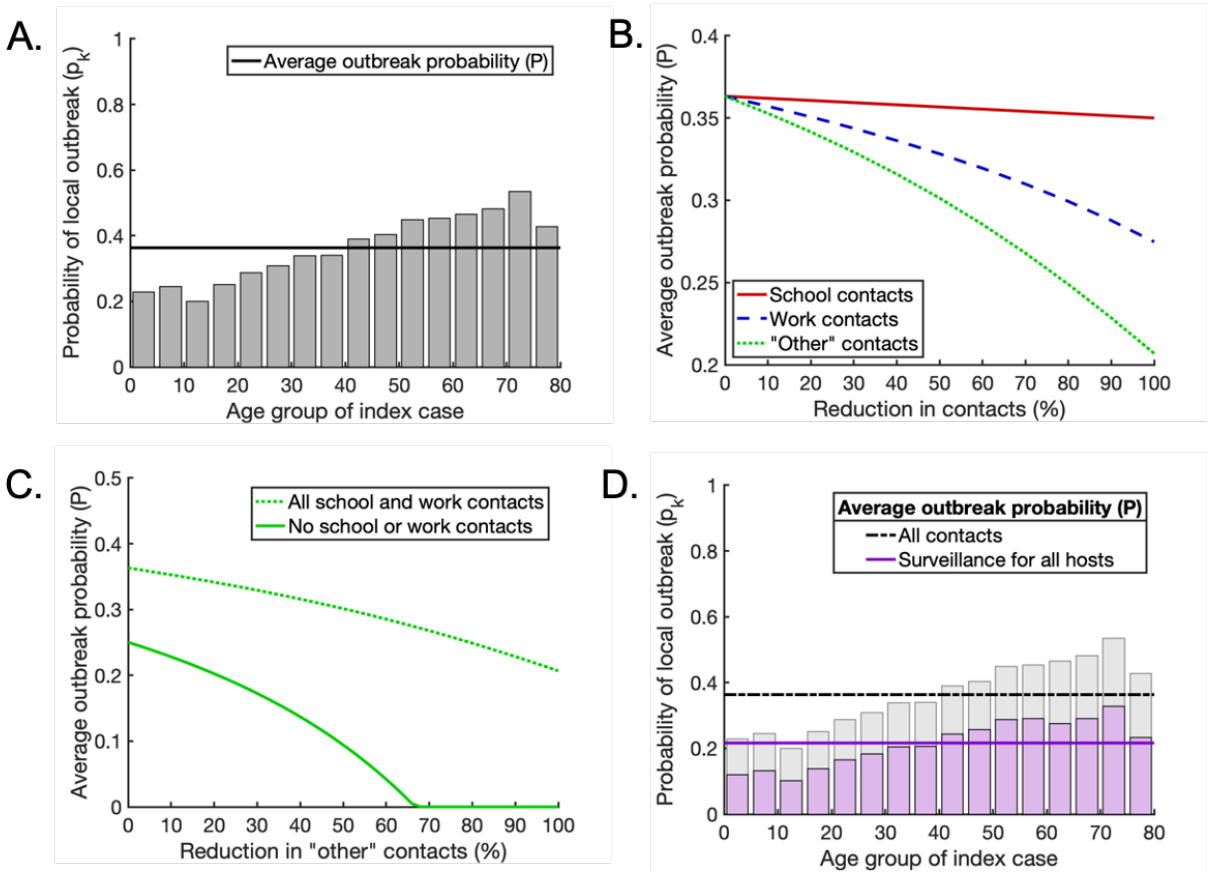

985 **Fig S10. Scenario C: The effect of increasing the proportion of infections that arise from**
986 **presymptomatic hosts from $K_p = 0.489$ (baseline value) to $K_p = 0.75$.** The proportions of infections
987 arising from symptomatic and asymptomatic hosts are adjusted so that they remain in the same ratio as in
988 the baseline case. For scenario C, both susceptibility to infection and the proportion of hosts who
989 experience a fully asymptomatic course of infection vary with age. A. Analogous to Fig 3C in the main
990 text: the probability that a single infected individual in any given age group triggers a local outbreak (grey
991 bars) and the weighted average local outbreak probability P (black horizontal line). B. Analogous to Fig 4D
992 in the main text: partial reductions in 'school', 'work' and 'other' contacts, and the resulting reductions in
993 the average local outbreak probability P (solid red, dashed blue and dotted green lines respectively). C.
994 Analogous to Fig 5D in the main text: the effect of reducing 'other' contacts on the average local outbreak
995 probability when 'school' and 'work' contacts are not reduced at all (dotted line) and when 'school' and
996 'work' contacts are reduced by 100% (solid line). D. Analogous to Fig 6E in the main text: the age-
997 dependent probability of a local outbreak with enhanced surveillance of both symptomatic and
998 nonsymptomatic infected hosts ($\rho_k = 1/2$ days^{-1} and $\sigma_k = 1/7$ days^{-1}), without contact-reducing NPIs
999 (purple bars and solid line). Pale grey bars and black dash-dotted line represent the local outbreak
1000 probabilities without any contact-reducing NPIs or enhanced surveillance (as in Fig S10A).
1001

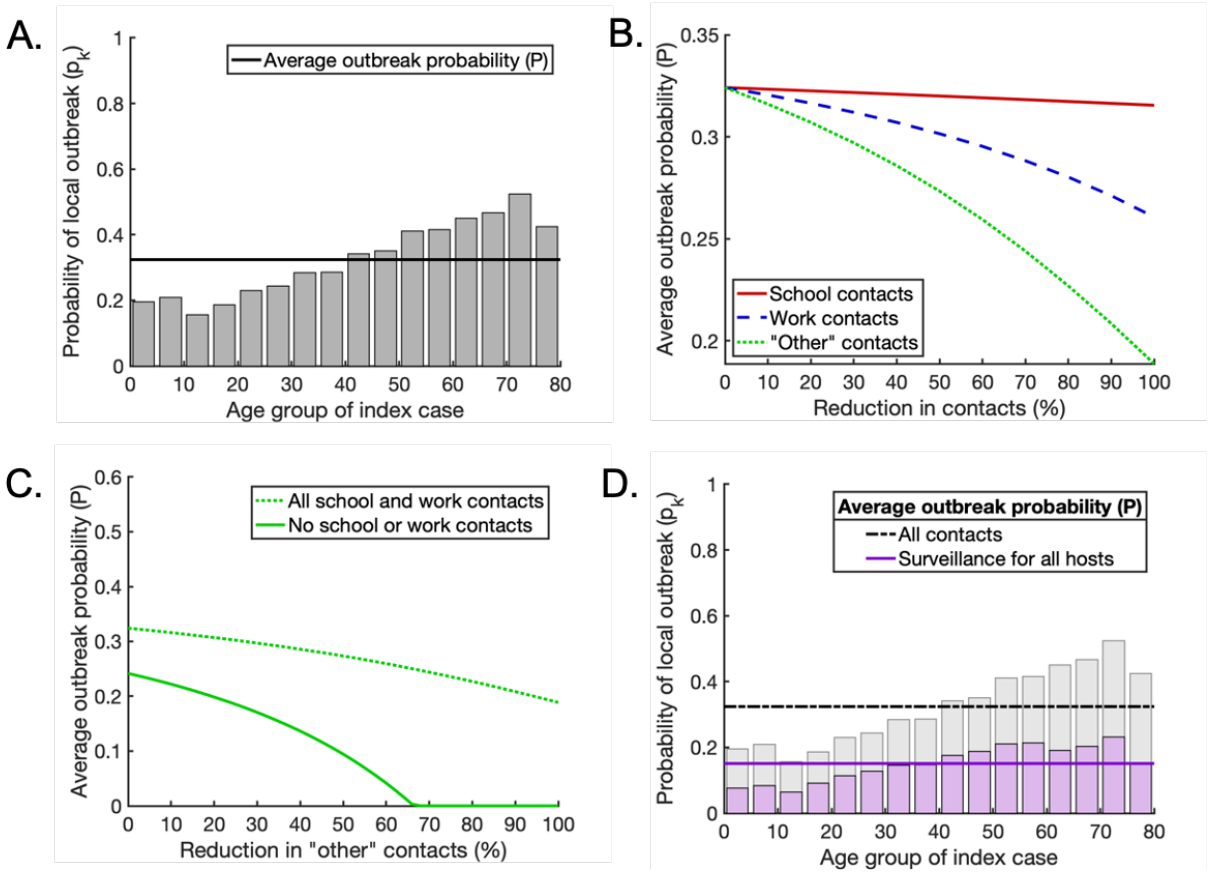

Fig S11. Scenario C: The effect of reducing the proportion of infections that arise from asymptomatic hosts from $K_a = 0.106$ (baseline value) to $K_a = 0.01$. The proportions of infections arising from symptomatic and presymptomatic hosts are adjusted so that they remain in the same ratio as in the baseline case. For scenario C, both susceptibility to infection and the proportion of hosts who experience a fully asymptomatic course of infection vary with age. A. Analogous to Fig 3C in the main text: the probability that a single infected individual in any given age group triggers a local outbreak (grey bars) and the weighted average local outbreak probability *P* (black horizontal line). B. Analogous to Fig 4D in the main text: partial reductions in 'school', 'work' and 'other' contacts, and the resulting reductions in the average local outbreak probability *P* (solid red, dashed blue and dotted green lines respectively). C. Analogous to Fig 5D in the main text: the effect of reducing 'other' contacts on the average local outbreak probability when 'school' and 'work' contacts are not reduced at all (dotted line) and when 'school' and 'work' contacts are reduced by 100% (solid line). D. Analogous to Fig 6E in the main text: the age-dependent probability of a local outbreak with enhanced surveillance of both symptomatic and nonsymptomatic

infected hosts ($\rho_k = 1/2$ days^{-1} and $\sigma_k = 1/7$ days^{-1}), without contact-reducing NPIs (purple bars and solid line). Pale grey bars and black dash-dotted line represent the local outbreak probabilities without any contact-reducing NPIs or enhanced surveillance (as in Fig S11A).

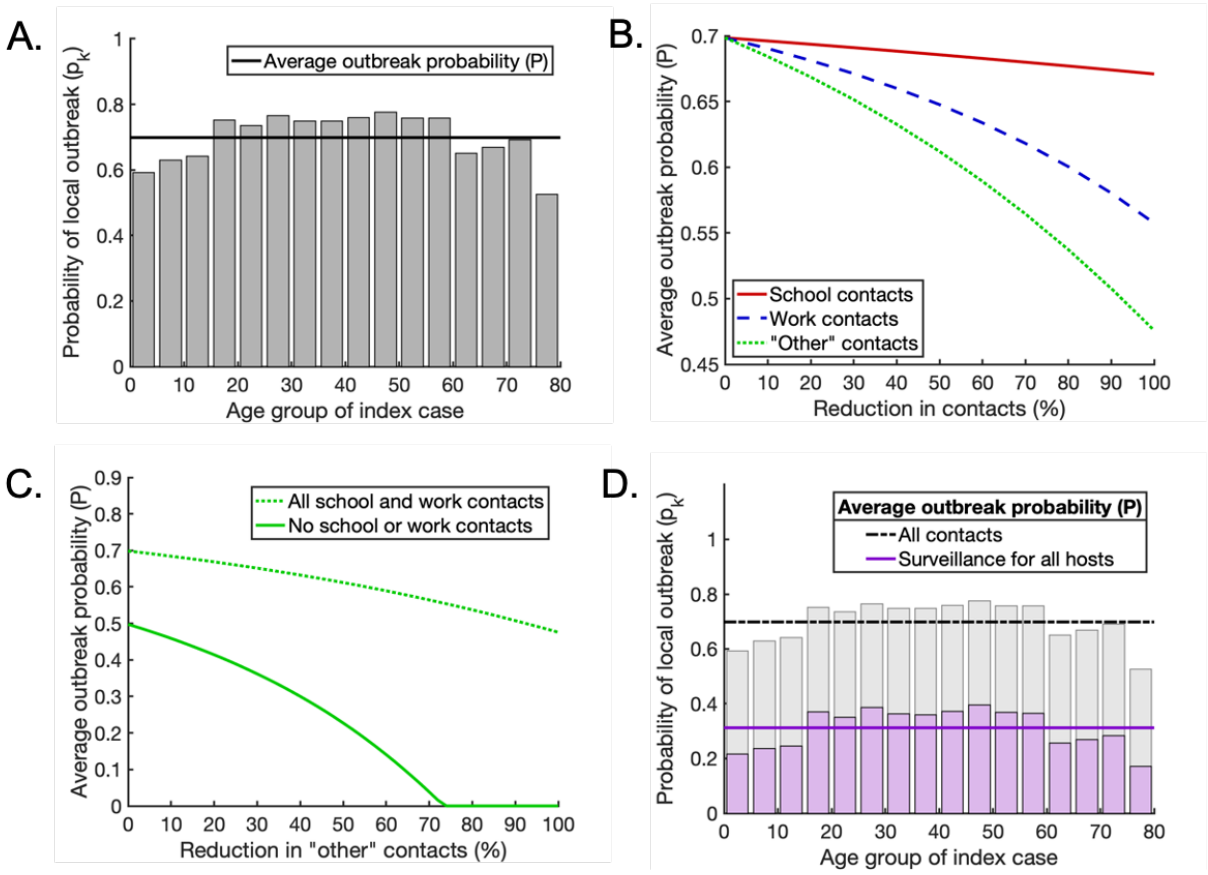

Fig S12. Scenario C: The effect of increasing the proportion of infections that arise from asymptomatic hosts from $K_a = 0.106$ (baseline value) to $K_a = 0.5$. The proportions of infections arising from symptomatic and presymptomatic hosts are adjusted so that they remain in the same ratio as in the baseline case. For scenario C, both susceptibility to infection and the proportion of hosts who experience a fully asymptomatic course of infection vary with age. A. Analogous to Fig 3C in the main text: the probability that a single infected individual in any given age group triggers a local outbreak (grey bars) and the weighted average local outbreak probability *P* (black horizontal line). B. Analogous to Fig 4D in the main text: partial reductions in 'school', 'work' and 'other' contacts, and the resulting reductions in the average local outbreak probability *P* (solid red, dashed blue and dotted green lines respectively). C.

Analogous to Fig 5D in the main text: the effect of reducing 'other' contacts on the average local outbreak probability when 'school' and 'work' contacts are not reduced at all (dotted line) and when 'school' and 'work' contacts are reduced by 100% (solid line). D. Analogous to Fig 6E in the main text: the age-dependent probability of a local outbreak with enhanced surveillance of both symptomatic and nonsymptomatic infected hosts ($\rho_k = 1/2$ days^{-1} and $\sigma_k = 1/7$ days^{-1}), without contact-reducing NPIs (purple bars and solid line). Pale grey bars and black dash-dotted line represent the local outbreak probabilities without any contact-reducing NPIs or enhanced surveillance (as in Fig S12A).